Lawrence Berkeley National Laboratory
Recent Work

Title

STUDIES ON ELECTRONICALLY EXCITED METASTABLE STATES OF MOLECULES WITH AN ULTRAHIGH-VACUUM MOLECULAR BEAM APPARATUS

Permalink

https://escholarship.org/uc/item/5bs0j8nj

Authors

Clampitt, R.
Newton, Amos S.

Publication Date

1967-12-01

ey. 2

University of California

Ernest O. Lawrence
Radiation Laboratory

STUDIES ON ELECTRONICALLY EXCITED METASTABLE STATES
OF MOLECULES WITH AN ULTRAHIGH-VACUUM
MOLECULAR BEAM APPARATUS

R. Clampitt and Amos S. Newton

December 1967

UCRL-18032 ey. I

DISCLAIMER

UNIVERSITY OF CALIFORNIA

Lawrence Radiation Laboratory
Berkeley, California

·

STUDIES ON ELECTRONICALLY EXCITED METASTABLE STATES OF MOLECULES WITH AN ULTRAHIGH-VACUUM MOLECULAR BEAM APPARATUS

R. Clampitt and Amos S. Newton

December 1967

STUDIES ON ELECTRONICALLY EXCITED METASTABLE STATES
OF MOLECULES WITH AN ULTRAHIGH-VACUUM
MOLECULAR BEAM APPARATUS[*]

R. Clampitt[†] and Amos S. Newton

Lawrence Radiation Laboratory
University of California
Berkeley, California

December 1967

ABSTRACT

A molecular beam apparatus designed for studies on metastable excited states of molecules is described. A molecular beam is crossed by an electron beam to produce electronically excited molecules. These pass into a chamber, operating at ultrahigh vacuum, and are detected by electron ejection from the surface of a photosensitive cathode, Cs_3Sb. The use of a 931A photomultiplier, without its glass envelope, for the detection of excited molecules is described. The detection of photons, positive ions and metastable molecules by time resolution and pulse counting techniques is described. Some results are presented on the effects of different surfaces on the efficienty of detection of excited molecules. Measurements were made on Kr, Ne, N_2, CO, CO_2, H_2, N_2O and C_2H_4. Electronically excited fragments from N_2O and CO_2 were detected and their threshold energies determined. A prominent resonant state of carbon monoxide at 10.5 eV is reported.

I. INTRODUCTION

The possibility that an excited atom or molecule might eject an electron from a metal surface was first suggested by Schottky[1] and was subsequently verified, accidentally, by Webb.[2] Up to the present only a few studies on metastable states using the method of electron ejection for detection have been made.[3-9]

The object of the work presented here was to extend that carried out previously in this Laboratory.[5] In particular, the apparatus to be described has allowed extension of the previous work by use of an alkali metal surface in an ultrahigh vacuum for the detection of long-lived excited states of molecules. The results obtained so far are limited to simple molecules, but they have indicated that the apparatus is equally suitable for studies on excited states of polyatomic molecules.

II. APPARATUS

A. General Description

The apparatus is shown schematically in Fig. 1. Gas effuses from chamber A through a slit G, 1.2 cm long and 0.023 cm wide, into chamber B, which is pumped by a liquid-nitrogen-trapped oil diffusion pump ($\approx$ 1200 liters sec^{-1}). The beam, modulated by a chopper, E, is further collimated by the slit H and passes into the excitation chamber C, pumped by a well-trapped oil diffusion pump[10] (1500 liters sec^{-1}). The beam is intercepted by an electron beam from an electron gun (F,J) and then passes through a slit K, 0.2 cm wide, used solely to aid differential pumping, into the detection chamber D, where it impinges on the detector P. Chambers C and D are constructed from Type 304 stainless steel and, together with the components therein, can be baked to 450°C.

The electron gun is shown to scale in Fig. 2. It consists of a directly heated cathode of thorium oxide coated on iridium, a shield slit, (1 × 0.1 cm), three focusing grids made of gold-plated tungsten mesh of 98% transparency, a graphite-coated collision chamber, and an electron collector. The electrons are confined by a magnetic field of $\approx$ 150 gauss applied externally. Considerable shielding of the filament is necessary to prevent light from reaching the photo-sensitive detector. Focusing grids of mesh were chosen in preference to slits to minimize spurious secondary electron currents resulting from electron scattering at slit edges.[11] The overall transmission of electrons to the anode is 12% at 12 eV. Two deflection plates M (see Fig. 1) were incorporated to prevent ions from reaching the detector. In this electron gun, the collision chamber is at the voltage of the electron energy and the filament is at ground potential.

The electron gun is aligned with slits G and H by adjusting internally its movable supports (Fig. 2). The alignment is check by focusing a telescope through slit K (Fig. 1) onto a flashlight bulb N, shielded to transmit light only in the direction of the slit G. Slits H and G are adjustable externally with a micrometer adjustment. Slit G can also be rotated about its axis. The chopper E[12] consists of two slotted vanes driven in opposition by an electro-magnet, and produces a trapezoidal-shaped slit of 1 msec duration, at a repetition rate of 200 Hz.

The detection chamber D is pumped by a liquid-helium-cooled surface rated at ≈ 1000 liter sec^{-1} for H_2 at $\leq 1 \times 10^{-8}$ torr.[13] The cryosorptive surface is a zeolite bonded to the outer surface of a cylindrical stainless steel reservioir filled with liquid helium (4.2 liters capacity.) Liquid-nitrogen-cooled baffles above the helium reservoir and a similarly cooled Dewar surrounding the vacuum wall minimize heat transfer to the surface. One charge of liquid helium lasts for 6 to 7 hours, and, after thermal equilibirum is established, for considerably longer periods.

A nude ion gauge[14] monitors the pressure, and a quadrupole mass filter[15] detects the residual constituents in the detection chamber. A bakeable bellows (see Fig. 1) provides linear movement of the detector over the range 10 to 20 cm from the electron beam. Modulated light from a monochromator at a quartz window (H, Fig. 3) in the detection chamber is used to measure the sensitivity and spectra response of the detector.

Preliminary evacuation of the apparatus is achieved with an external liquid-nitrogen-cooled cryosorption pump to avoid contamination of the detector chamber with pump oil. After thorough evacuation and 20 hours baking of chambers C and D at 250° C the pressure in the detection chamber is reduced to

between 6×10^{-11} and 1×10^{-10} torr, and consists mainly of H_2, CO, and CH_4. The pressure in the detection chamber in the presence of a molecular beam ($\approx 10^{13}$ molecules/sec) varies with the nature and intensity of the beam. In the presence of beams of H_2, N_2O, and C_2H_4, for example, the equilibrium pressure was about 4 to 6×10^{-9} torr.

B.   Detectors

The method of detection of the electronically excited species involves the ejection of electrons from a metal surface by the impinging molecule. Surfaces of the alkali metals make highly efficient detectors because of their relatively low work functions, and have been used previously by several workers.[6,16] However, the useful lifetime of such surfaces in systems not prepared and designed to maintain an ultrahigh vacuum varies between half an hour and several hours.[17] In the present apparatus surfaces of cesium and cesium antimonide can be maintained active for several months in the presence of beams such as N_2, CO, CO_2, C_2H_4, H_2, and C_3H_6 without any significant decrease in photosensitivity. Two types of cesium-coated electron multiplier have been used successfully: one was a 16-stage windowless electron multiplier,[18] the cathode of which was coated with a film of antimony. This had a gain of $\approx 1 \times 10^5$ at 2000 V and was used to study abundant metastable species such as Kr, N_2, and Ar. To further increase its gain and sensitivity to metastable molecules, a film of cesium was deposited on the cathode in the following way: the cathode was heated by radiation from a tungsten filament in close proximity; then a slotted nickel tube containing a mixture of cesium chromate and silicon was heated to 700 to 800°C, and cesium was formed and effused onto the cathode.

The deposition was continued until there was no further increase in the photo-electric response of the cathode (about 3 min). An increase of ≈ 100 in sensitivity to metastable N_2 molecules having 12 eV of electronic excitation was observed.

The method described above, cesium deposition in situ, is not an efficient way of producing a cesium-coated surface, since any cesium that does not adhere on the first collision with the surface is lost to the walls of the chamber. The method used by manufacturers of photomultiplier tubes is more elegant: cesium at a pressure of $\approx 10^{-2}$ torr is produced in a closed phototube; the temperature of the reaction (Cs + Sb) is controlled and the spectral response and resistance of the film are continuously monitored. Consequently the manufacturer can produce photocathodes of known chemical composition, surface structure, and spectral sensitivity. It was advantageous, therefore, to use such a previously prepared multiplier for the detection of metastable molecules, and to adapt it to our purposes by removing its vacuum envelope inside the evacuated detection chamber. An RCA nine-stage 931A photomultiplier having an S-4 response was used. The photomultipliers were obtained from the manufacturer without the Bakelite pin base. All the dynodes were covered with cesium antimonide, giving a typical gain of 1×10^5 at 1000 V. Unlike most other photomultipliers, this type does not have its photocathode deposited on the glass envelope, the removal of which, therefore, does not affect its performance. During the baking of the system the multiplier must be kept cool, otherwise serious loss of Cs from the dynodes will occur. Cold water is passed through the hollow finger (Fig. 3).

The method of removal of the vacuum envelope in vacuum is simple and inexpensive: a hot wire cracks the glass, which falls into a bucket. Figure 3 shows the photomultiplier in position. The spectral response curve (S-4) was

first measured by using modulated light from a monochromator at the quartz
window, H, and with the photomultiplier coupled to a lock-in amplifier. The
use of the monochromator serves also to study the stability of the Cs_3Sb photo-
cathode A during the impingement of a molecular beam; a scan over the spectral
range 300 to 700 mμ can be recorded in a few seconds by driving the diffraction
grating mechanically. The glass envelope was not removed until the pressure
was down to $\leq 2 \times 10^{-10}$ torr in the detection chamber; and the residual gases,
as analyzed with a quadrupole mass filter, were devoid of O_2 and water. The
multiplier was clamped in a holder near its base, and a 500-g copper weight D
was suspended from the envelope by means of several steel wires C. A nichrome
wire, previously outgassed, and in contact with a diamond-etched mark on the
glass, was heated rapidly, to break the envelope, which then fell with the
copper weight into bucket J above the liquid helium pump. The envelope does
not fall without the encouragement of a weight partly because it is held to
the multiplier by metal spacers. The spectral response curve in the visible
region of the spectrum for the photomultiplier remained unchanged when the en-
velope was removed. It was found that the glass envelope had a transmission
of 65% at 550 mμ.

The support F is a hollow tube that can be filled with liquid nitrogen
to cool the multiplier. A shield E surrounds the multiplier and is operated at
a potential selected for minimum noise current; it can also be used to prevent
ions from reaching the multiplier.

C. Performance of the Electron Gun

In order to study fine structure in the excitation functions of molecules
to metastable states it is necessary to use an electron beam of well-defined
energy. The electron gun used here is a modification of that developed by Fox,
Hickam, Grove, and Kjeldaas,[19] which utilizes the so-called retarding-potential-
difference (RPD) method of producing beams of pseudomonoenergetic electrons.
The electrons emitted by the filament are accelerated through focusing grids to
a cutoff grid, the potential of which is about 0.5 V negative with respect to
the filament. This cutoff potential yields a sharp low-energy cutoff point in
the electron energy distribution. Further acceleration to the collision chamber
gives a distribution at that point, of energy eV, with a sharp low-energy cutoff.
A small sine or square wave of about 0.2 V is applied to the negatively biased
grid at a frequency selected for minimum noise in the detector circuit. At
the collision chamber the distribution has low-energy cutoffs of eV and
$e(V + 0.2)$ which vary at the modulation frequency. If the detector is modulated
at the same frequency with a lock-in amplifier,[20] the resulting difference
signal is due to those molecules excited by electrons of energy spread of 0.2 eV
at an energy eV. This is a close approximation to a monoenergetic beam.

The electron current at the anode of the electron gun was about 0.2 μA.
The method was tested by observing the sharp resonant states of neon $2p^5 3s$
(16.62 eV) and $2p^5 3p$ (18.38 eV), and also by reproducing the sharp resonant-
peak $E^3\Sigma_g^+$ state at its maximum at 12.1 eV in N_2. An excitation curve for
nitrogen is shown in Fig. 24. These resonant peaks were sufficiently sharp
that the electron energy resolution was considered satisfactory.

If a small sine wave is applied to a slowly varying potential on the
electron accelerating grid, the first differential of the excitation function
can be obtained. The effect of modulating the accelerating voltage is to
differentiate the signal. In Fig. 22 the first differential of the nitrogen
excitation curve is shown. The differential output signal is displayed on the
y axis of an x-y recorder, with the electron accerlerating voltage displayed
on the x axis.

Deflection plates M, beyond the electron gun, are used to remove ions
from the beam. One plate is normally grounded and the other is maintained at
about -30 V. It was found that if the latter plate was made highly positive
with respect to ground (> +40 V), then electrons scattered out of the collision
chamber by the molecular beam are further accelerated forward from the posi-
tively charged deflector plate and collide with molecules of the beam to pro-
duce additional excitation. For hydrogen it was shown that a significant
number of photons were produced in this way when the deflector plate was
positively charged.

Since the detector responds to visible light, considerable care must be
taken to shield the filament of the electron gun. The ion gauge and mass filter,
situated in the detection chamber, are not operated when the photomultiplier is
in operation because of interference from the light they produce.

D. Alignment of the Molecular Beam

As mentioned previously, the slits in chambers A and B and in the colli-
sion chamber are aligned initially by using a telescope focused on the light
from the flashlight bulb (N, Fig. 1) in chamber A. They are aligned further,
under vacuum, by modulating this light with the chopper and detecting the
200 Hz component of the photomultiplier current with a lock-in amplifier. The
photomultiplier can be moved in both the lateral and vertical planes of Fig. 1
by means of screw adjustments on a steel table to which the bellows is
attached. Adjustments are made until it is found that the light signal from
chamber A does not vary when the multiplier is moved from a minimum distance
of 10 cm to a maximum distance, 20 cm from the electron gun. The photocathode
of the multiplier is 2.5 cm long and 1 cm wide. At the detector, the molecular
beam width is 0.6 cm, and its height 1 cm, therefore a correctly aligned photo-
multiplier collects all the light or molecular beam. This alignment is critical
for measurements on the decay of metastable species with distance (time) from
the electron gun. A final alignment of the electron beam with respect to the
molecular beam is made by adjusting the position of its collimating magnet for
maximum signal of metastable molecules at the detector.

III. METHODS OF DETECTION

A. Modulation Techniques

The molecular beam can be modulated at 200 Hz and the modulated com-
ponent detected with a frequency-sensitive amplifier locked in phase with a
reference sine wave derived from the mechanical chopper. This method discri-
minates considerably against noise and background gas.

The electron beam can be modulated for operation in the RPD mode and
the modulated metastable component detected as above. This method does not
discriminate against the signal from the background gas, which is also modu-
lated at the electron beam frequency. Consequently, for studies on the variation
in yield of metastable species with detector distance, it is advantageous to
employ mechanical modulation of the molecular beam, since under these conditions
only molecules excited within the beam are detected.

For the detection of very weak signals electron beam modulation is
superior to the mechanical method, since the frequency can be selected for
minimum noise level (usually > 600 Hz), whereas mechanical modulation was fixed
at 200 Hz.

B. Pulse-Counting Techniques

The photomultiplier can be operated in a pulse-counting mode for the
detection of photons, ions, and electronically excited molecules. The techni-
ques to be described are found to be superior, in almost every respect, to the
methods of modulation, and the versatility of the apparatus can be increased
considerably. Pulse-counting methods have facilitated the measurements of
(i) molecule velocity distributions and excitation functions, (ii) photon

contributions to the excitation function, (iii) excitation functions for the

production of photons, (iv) velocity distribution of electronically excited

neutral fragments formed with kinetic energy of dissociation, and (v) velocity

distribution of positive ions produced by the electron bombardment.

The photocathode of the 931A multiplier normally operates at negative

high voltage (typically - 1000 V). The cathode of the 16-stage multiplier is

operated at ground potential for minimum noise and therefore capacitive de-

coupling of the anode is necessary. The anode, near ground potential, is

coupled to a low-noise distributed amplifier having a gain of 5.[21] The noise

level can be further reduced by cooling the amplifier with liquid nitrogen.

Three additional amplifiers make a total gain of about 12000. The noise

passed by the discriminator amounts to 1 to 2 counts/sec.

1. Excitation Functions of Metastable Molecules

Excitation functions of metastable molecules can be obtained as follows:

The electron gun is operated as a dc source of electrons. A ramp (sawtooth)

generator is used to sweep the electron accelerating voltage over the desired

range at a selected rate, typically 250 Hz. A trigger pulse, synchronized in

time with the start of the sweep, triggers a programmed time-base oscillator

and also starts a multichannel analyzer operated in the multiscaler mode. The

residence time per channel, preselected with the time-base oscillator, is chosen

such that the total time required to store counts in 100 channels is exactly

equal to the time required to sweep the electron energy range. Due allowance

must be made for the memory-recovery time of each channel ($\approx$ 12 μsec). The

minimum residence time for each channel is 10 μsec, and so the fastest sweep

that can be obtained in this mode is $\approx$ 2.2 msec. Repetitive sweeps of the

electron energy are made to achieve a satisfactory signal-to-noise ratio (this amounts to several seconds for Kr and several minutes for H_2). The electron current can be monitored on a dc microammeter or displayed on the analyzer by means of a voltage-to-pulse-frequency converter.

Photons and metastable molecules cannot be distinguished by this method; to do this the technique of delayed coincidence counting described below was used.

2.   Delayed Coincidence Counting

The electron gun is operated in the pulsed mode. The electron current from the filament is cut off at a grid. A positive square-wave pulse of 2 to 3 V amplitude and 10 μsec width is then applied to the grid to provide pulses of electrons. The scheme is shown in Fig. 4. The time lapse between pulses is chosen to be greater than that required for all of the resultant metastable molecules to arrive at the detector (≈ 0.4 msec for Kr). Another pulse, sychronized with the electron beam pulse, triggers a coincidence gate following the discriminator. When this pulse is not delayed only photons are counted (provided that its width is only ≈ 10 μsec). If the gate pulse is delayed for an appropriate period only metastable molecules are counted. The analyzer is triggered, as previously, to start storage at the beginning of the ramp sweep of the electron acceleration voltage.

3.   Time-of-Flight Measurements

a.   Multiscaler mode. The analyzer is triggered, via the time-base oscillator, to start storage at the onset of the electron beam pulse. The minimum storage time per channel that can be obtained is 10 μsec; this, to- gether with ≈ 12 μsec dead time per channel, means that at least 2.2 msec are

required in order to store counts in 100 channels. For metastable molecules of

high mass such as Kr this is satisfactory; for H_2, and kinetically energetic

fragments, the counts are bunched in the first few channels, and for these

species measurements of velocity are difficult and inaccurate. Figure 5 shows

the velocity distribution of Kr obtained with 13-eV electrons.

    b. <u>Pulse-height mode</u>. In order to sample species much earlier after

electron beam excitation the scheme shown in Fig. 6 was used. The essential

component is a time-to-pulse-height converter. Pulses from the amplifiers are

shaped and stretched to $\approx$ 100 nsec by the discriminator and pass into a linear

gate, which, when fed with a ramp signal, generates pulses the amplitudes of

which are proportional to the amplitude of the ramp. In this particular device

ramp sweeps of 10 μsec to 50 msec can be selected. The ramp and linear gate

are triggered by the electron beam pulse. Any signal pulse arriving after the

start of the ramp produces an output pulse from the linear gate of amplitude

proportional to its time of arrival. A Schmitt trigger stops the ramp and

closes the control gate. The process is repeated at the frequency of the

electron pulse, typically 1000 Hz. The analyzer is used in the pulse-height

mode and so does not limit the sampling time as in the multiscaler mode. When

100 channels are used the fastest sweep time that can be obtained with the

present apparatus is 1 μsec.

    With this technique it is possible to study the profiles of the velocity

distribution curves for fast metastable species such as H_2^*, or an energetic

fragment of a molecule that cannot be satisfactorily resolved in the multiscaler

mode. Also, by operating the collision chamber at 15 to 30 eV above ground

potential the time-of-flight spectrum of ions can be produced. Figure 7 shows

a 400-μsec scan of photons, ions, and metastable atoms from neon. A useful

study by this method could be made on the kinetic energy of fragment ions from diatomic or triatomic molecules. For molecules containing more than three atoms the spectra would probably be too complicated. The time-of-flight distribution of protons from electron bombardment of H_2 is shown in Fig. 8. It is seen that there are many groups of protons formed with different amounts of kinetic energy. Figure 9 shows the time-of-flight spectrum of N_2O^+ and its fragment ions.

It is possible also to obtain separate excitation functions for the production of photons, fragment ions, molecular ions, and metastable molecules resulting from a single molecular species. Figure 10 shows a hypothetical time-of-flight distribution of species produced from a triatomic molecule. To obtain separate excitation functions for these, the method of delayed coincidence (Sec. IIIB2) is used in conjunction with the pulse-height mode. The pulses to the coincidence gate are represented in Fig. 10 by the square waves numbered 1 to 7. First, a time-of-flight curve is obtained by the pulse-height method and the time of arrival of the various species determined. The coincidence gate is delayed to correspond in time with the arrival of the selected species. Then the threshold energy is determined as in Sec. IIIB2. The excitation function can be readily determined for fragment ions formed without a significant amount of kinetic energy, since their time of arrival does not vary with electron bombarding energy. The collision chamber is maintained at + 20 V and the filament potential varied to give the desired electron energy. The yield as a function of electron bombarding energy of ions having a particular value of kinetic energy can be obtained by choosing the appropriate delay time. This method is similar to the retarding-potential method used in mass spectrometry, but it is superior, since, in the latter method, all ions above a certain kinetic energy are counted.

IV. EXPERIMENTAL RESULTS

A. Density Distribution Through the Mechanical Chopper

The shape of the slit produced by the mechanical chopper in chamber B (Fig. 1) can be obtained by using the analyzer in the multiscaler mode to display the light-count rate from the source N as a function of time. A square wave used to start the analyzer is phase-locked to a reference sine wave derived from the mechanical chopper.

The density distribution of light through the trapezoidal-shaped slit is shown in Fig. 11. The average open time of the chopper is 1 msec. Figure 12 shows the density distribution of metastable krypton atoms obtained by phase-locking the electron beam pulse to the sine wave. The dotted curve is the theoretical distribution for a rectangular slit calculated from the equations,

$$N(t) = \frac{\pi^{1/2} I_o}{2d} \left[1 + \frac{2}{\pi^{1/2}} \frac{d}{\alpha t} \exp\left(\frac{-d^2}{\alpha^2 t^2}\right) - \mathrm{erf}\left(\frac{d}{\alpha t}\right) \right] \tag{1}$$

for $t \leq t_o$, and

$$N(t) = I_o \left[\frac{2}{\pi^{1/2}} \frac{d}{\alpha t} \exp\left(\frac{-d^2}{\alpha^2 t^2}\right) \frac{-2a}{\pi^{1/2}} \exp(-a^2) - \mathrm{erf}\left(\frac{d}{\alpha t}\right) + \mathrm{erf}(a) \right] \tag{2}$$

for $t \geq t_o$, where t_o is the open time of the chopper, I_o is the total number of molecules, d is the distance from the chopper to the detector, α is the most probable velocity; erf(x) is the error function and a is defined by

$$a = \left(\frac{\alpha t}{d} - \frac{\alpha t_o}{d} \right)^{-1}$$

B. Velocity Distribution of Metastable Species

To determine accurately the velocity distribution of excited molecules of mass $\geq$ 20 amu the multiscaler mode can be used. The velocity distribution of molecules in a molecular beam is given by

$$N(v)dv = \frac{2I_o \, v^3}{\alpha^4} \, \exp(-v^2/\alpha^2) \, dv \qquad , \qquad\qquad (3)$$

since the probability of effusion is proportional to velocity. However, since the probability of electron excitation is proportional to molecular density and thus inversely proportional to molecular velocity, the velocity distribution of molecules excited by electron impact reverts to a v^2 distribution. The number of metastable molecules excited by a pulse of length Δt arriving at the detector between the interval t and $(t + dt)$ is given by

$$N(t)dt = \frac{2I_o \, \Delta t \, d^3}{(\alpha t)^4} \, \exp\left(\frac{-d^2}{\alpha^2 t^2}\right) \, dt \qquad , \qquad\qquad (4)$$

since $\frac{dv}{dt} = \frac{v^2}{d}$. Equation 4 is applicable when $\tau \geq 10^{-2}$ sec.

The fraction of molecules arriving later than t is given by the integral of Eq. 4 between the limits t and ∞ .

An experimental velocity distribution is shown in Fig. 12a together with a theoretical curve derived from Eq. 4. The poor fit on the low-velocity side of the curve might be partly because the electron beam pulse is not a sharp square wave.

C. Dead Time of the Analyzer

The inherent dead (or memory) time per channel of the analyzer operated in the multiscaler mode is $\approx$ 12 μsec. Accurate dead times of 20 μsec and longer can be selected by the programmed time-base oscillator. The average inherent dead time can be conveniently estimated by noting the channel at which the peak in a velocity distribution occurs for a selected dead time (for example, 20 μsec). The distribution is again measured without a fixed dead time--that is, utilizing the inherent dead time only. The average inherent dead time can then be calculated from the displacement in time of the peak. A value of 13.3 $\pm$ 0.5 μsec was obtained for the analyzer used in this work.

D. Simultaneous Counting of
Photons, Ions, and Excited Neutral Species

A time-of-flight distribution of photons, ions, and metastable atoms from neon, obtained by the method of Sec. IIIB3b, is shown in Fig. 7. Photon and ion spectra for H_2 and N_2O are shown in Figs. 8 and 9 respectively. The curves for H_2 show a prominent thermal H^+ group and several groups of energetic protons, one of very sharply defined kinetic energy. Detection of kinetic energy in fragment ions from N_2O is made difficult by the presence of many fragments.

The N^+ fragments from N_2 produced at 24 eV bombarding energy consist of a thermal group and one or more energetic groups (Fig. 13). At 35 eV very few thermal ions are formed (Fig. 14).

E.   Velocity Distributions and Threshold Energies
of Fast Metastable Species

1. Nitrous Oxide

Freund and Klemperer,[7] using a technique similar to the one used here,
found that the excited species produced by electron bombardment of N_2O was formed
with excess kinetic energy, and was therefore an excited neutral fragment. The
method described in Sec. IIIB3b was used to obtain an accurate velocity distri-
bution and is shown in Fig. 15. Over the electron energy range 15 to 40 eV
the most probable velocity does not vary by more than $\approx 1 \times 10^4$ cm/sec, which
suggests that the repulsive potential energy curve describing the dissociation
is shallow. The threshold energy for the production of this fragment, obtained
with 0.02 μA of electrons, is 10.5 ± 0.3 V. This value is higher than the pre-
viously reported value of 8.7 eV obtained with 80 mA of electrons.[7]

If it is postulated that the excitation process leading to the observed
fragment involves a change of electron spin, then the following processes can
occur:

(i) $N_2O \longrightarrow N_2(a^1\Pi_g) + O(^3P)$ ....10.26 eV

(ii) $N_2O \longrightarrow NO(A^2\Sigma^+) + N(^4S)$ ....10.37 eV

(iii) $N_2O \longrightarrow NO(B^2\Pi_r) + N(^4S)$ ....10.62 eV

(iv) $N_2O \longrightarrow N_2(B^3\Pi_g) + O(^1D)$ ....11.03 eV
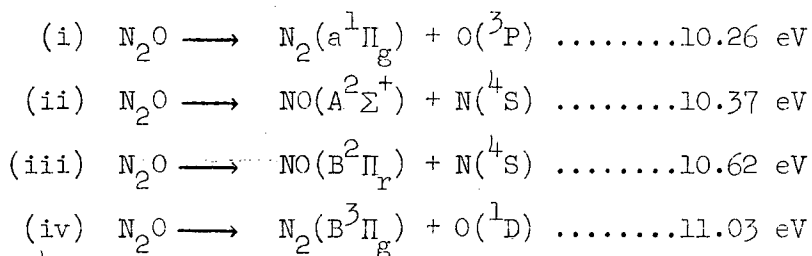
The excited species is not polar, since it is not deflected by an inhomogeneous
electric field,[7] and so it is almost certainly N_2. The lifetime of $N_2(B^3\Pi_g)$
is $\approx 10^{-6}$ sec; $N_2(a^1\Pi_g)$ of process (i) would be formed with 0.3 eV of kinetic
energy and has a lifetime of $\approx 10^{-3}$ sec. The threshold value for process (i)
is close to the observed value. The measured kinetic energy of the excited

species, assuming it to be N_2, is 0.43 ± 0.02 eV at 15 eV bombarding energy. We suggest, therefore, that the excited fragment produced by electron bombardment on N_2O is $N_2(a^1\Pi_g)$.

2. Carbon Dioxide

An excited, energetic fragment from electron bombardment of CO_2 has also been reported recently.[7] The species, found to be polar, is almost certainly CO^*. The velocity distribution is shown in Fig. 16; it is seen that there is considerable photon emission from CO_2. Separate excitation functions were obtained for the production of photons and metastable fragments by using the method of delayed coincidence (Sec. III1B2); the threshold energies were determined by comparison the ionization potential of CO_2. The photon threshold was 10.0 ± 0.6 eV; the CO^* threshold 11.0 ± 0.6 eV, and it is formed with an average kinetic energy of 0.26 eV. Warmek[22] showed that the photolysis of CO_2 produces CO and $O(^1D)$. He proposed the existence of an excited state of CO_2 which at low pressures either predissociates or reemits a photon. However, because of the spin-conservation rule in photon absorption, it is likely that the excited state leading to the fragment observed here and previously[7] is not that one produced in the photolysis of CO_2.

3. Hydrogen

The production rate of photons from electron impact on H_2 above 11 eV is far greater than that of metastable H_2 molecules. Figure 17 shows the time-of-flight distribution of photons and H_2^*. Figures 18 and 19 show the separate excitation curves. The threshold for the production of H_2^* is close to the spectroscopic value[23] of 11.86 eV. The curve exhibits a resonant character

and closely resembles that reported by Lichten,[8] using a magnetic deflection method, and by Cermak,[24] using the method of Penning ionization.

An excitation function reported previously in this Laboratory[5] differs considerably from the one in Fig. 18, most probably because no allowance was made for photon production.

Electron beam excitation of H_2 has been used as a source of metastable H(2S) atoms[25] ($\approx 10^{-4}$ torr H_2; 500-μA electrons). In the work reported here there was no evidence in the velocity distribution for the presence of metastable H(2S) atoms resulting from the repulsive $^1\Sigma_u^+$ state and others. Neither were photons observed when the beam was passed through an electrostatic field of $\approx$ 500 V/cm. The excitation cross sections at 15 eV electron energy for the production of H(2S) atoms and $c^3\Pi_u$ metastable molecules are, respectively, $\approx$ 0.08 (Ref. 26) and $\approx$ 10 (Ref. 27) in units of $\pi\alpha_o^2$. Since, under our experimental conditions ($\approx 10^{-7}$ torr H_2; 0.02 μA electrons) only a weak signal from H_2^* was observed, it is not surprising that no H(2S) atoms were detected.

F.   Observations on Some Other Metastable Species

1.   Carbon Monoxide

Previous experimental work on metastable states of carbon monoxide is scant. Lichten reported[9] a threshold energy of 6.2 eV. Olmsted, Newton, and Street[5] extended this work, using a pseudo-monoenergetic electron gun; they reported a threshold energy at 6.9 eV and a distinct break at $\approx$ 10.3 eV which coincides with the theoretical threshold energy for the $b^3\Sigma^+$ state. It was postulated that the signal appearing at 6.9 eV was due either to photons or to

the metastable $a^3\pi$ state of CO. Cermak also observed[24] a metastable state lying $\geq$ 10.2 eV above the ground electronic state. In the work reported here, when a Cs_3Sb detector was used, and delayed coincidence counting to eliminated photons, the threshold energy was observed to be 6.5 ± 0.3 eV by comparing it with the threshold for the production of metastable krypton (9.92 eV). Furthermore, a prominent resonant peak appears at 10.5 ± 0.3 eV (Fig. 20), and might well be due to the $b^3\Sigma^+$ state suggested previously.[5] The time-of-flight distribution of photons and CO^* is shown in Fig. 21.

The low-energy inelastic electron scattering spectrum of $CO^{28,29}$ exhibits a prominent resonant peak at $\approx$ 6 eV attributed to the $a^3\pi_r$ state, and a weaker one at 10.37 eV ($b^3\Sigma^+$). The latter is very close in energy to the peak at 10.5 eV observed here. The reported lifetime of the transition $a^3\Pi_r \rightarrow X^1\Sigma^+$ is about 10 μsec.[30] It must be longer than this.[31] Since all higher triplet states radiate by allowed transition to the $a^3\Pi$ state, the observed prominence at 10.5 eV may be fortuitous.

2. **Nitrogen: The Effects of Surface Composition on Excitation Functions**

Several workers have reported excitation functions for the production of metastable N_2 molecules, but there are considerable differences in the shapes of the curves. Three experiments, in particular, appear to resolve some of the differences. Cermak showed,[24] by a method of Penning ionization, that a state having a threshold energy E at $10.2 \leq E < 11.4$ eV exhibits a maximum cross section at $\approx$ 14 eV. Ehrhardt and Willman,[32] using a 127-deg electron velocity selector, showed that the cross section for excitation of N_2 to a state 11.03 eV above the ground state reached a maximum at $\approx$ 14 eV bombarding energy. This was attributed to the $C^3\Pi_u$ state. Stewart and Gabathuler[33] reported that the intensity of the second positive system of N_2 ($C^3\Pi_u \rightarrow B^3\Pi_g$) reaches a maximum

at ≈ 15 eV bombarding energy. These three experiments strongly suggest that the cross section for excitation of the $C^3\Pi_u$ state of N_2 by low-energy electrons does not reach a maximum until ≈ 4 eV above the threshold energy.

Previous experiments on the detection of metastable N_2 by electron ejection from a metal surface are not fully in accord. Lichten observed[9] a sharp peak at ≈ 12.2 eV and a broader one at ≈ 14.5 eV. Winters observed[34] three peaks at, respectively, 11.0, 12.0, and 14.0 eV. Olmsted, Newton, and Street[5] observed a sharp peak at 12.2 eV ($E^3\Sigma_g^+$); however, they did not report measurements above 13.2 eV. In the work presented here the shape of the excitation curve was shown to depend markedly on the nature of the surface used to detect the metastable molecules. It was proved that the photon contribution was negligible below 15 eV electron energy. Figures 22 through 24 show excitation functions for N_2 obtained by using (i) a vacuum-deposited film of antimony, (ii) a vacuum-deposited layer of cesium on an antimony film; composition unknown, and (iii) a Cs_3Sb surface having a S-4 photoelectric response.[35] Before cesium deposition (Fig. 22) only the $E^3\Sigma_g^+$ state at 12.2 eV is prominent, but on the cesium surface, two peaks at respectively, 11.0 and 14.0 eV become dominant.

It is futile to attempt an explanation of the differences in excitation functions simply on the basis of work functions, since in no case was the nature of the surface known. However, the work presented here shows unequivocally that the shape of an excitation function obtained by the method of electron ejection depends strongly on the nature of the surface. This has recently been discussed by Olmsted.[36] It appears also that for a given molecule the efficiency of electron ejection depends on the level of electronic excitation, or, rather, on the chemical and physical properties of the excited molecule.

For a cesium film (Fig. 23), another possibility arises. By analogy with Penning ionization of atoms in the gas phase, it is possible that Cs atoms, loosely bonded to the antimony surface, are ionized by the incoming metastable particle. The valence electron escapes but the ion is retained by the negative electric field at the cathode. The yield of electrons for metastable atoms of increasing excitation energy will thus reflect the shape of the ionization efficiency curve for the production of Cs^+. The ionization efficiency curve reported by Tate and Smith[37] for the process $Cs + e \rightarrow Cs^+ + 2e$ is shown in Fig. 22 inset. There are two distinct changes in yield, one at ≈ 10 eV and a larger one at 15 eV. These coincide almost exactly with the observed peaks in the excitation curve of N_2^* (Fig. 23).

Hence, although there is strong evidence for a maximum in the cross section of the $C^3\Pi_u$ state at 14 to 15 eV, the peak at this energy in Fig. 23 may not be a true representation of the shape of the excitation function for this state.

3. Ethylene

A very weak signal in ethylene was detected and required a counting time of 1 hour to obtain an excitation function. Even after this period the data were not adequate to confirm the distinguishing features previously observed by Lichten.[6] The time-of-flight distribution obtained at 17.2 eV showed a high photon count rate and a low metastable count rate. Unlike results for several other gases studied here, photon counts were observed up to 90 μsec after cutoff of the electron beam pulse; this might be due to emission from a short-lived metastable state of ethylene.

The threshold energy for the production of $C_2H_4^*$ was 9.5 ± 0.4 eV, and

for photons, 7.6 ± 0.5 eV. The excitation function reported by Lichten has a

threshold of ≈ 8 eV and a prominent resonant peak at ≈ 11 eV. The absence of

a signal below 7 eV is consistent with the absence of phosphorescence in ethylene,

but is in contrast with the assignment to a singlet-triplet transition of a

peak at ≈ 4.5 eV in the inelastic scattering spectrum of ethylene.[38,39]

4. Surface Ionization of Metastable Atoms at the Detector

If the Cs_3Sb cathode of the multiplier is biased positive with respect

to the second dynode, only positive ions, photons, and reflect neutral atoms

can reach the second dynode. A signal was detected at the anode when the cath-

ode, biased in this manner, was bombarded with a beam of Kr^* atoms; the

threshold for the process was 14 ± 1 eV. The threshold energies for the pro-

duction of Kr^* and Kr^+ are, respectively, 9.92 and 14.0 eV, and so it appears

that Kr^+ ions are produced at the cathode. When the cathode potential was

biased only 5 V positive with respect to the second dynode, no signal was

detected at the anode. If the species produced at the cathode were photons

or metastable atoms then the count rate would not have changed at all. That

the signal increases with increasing potential difference suggests the focusing

of positively charged ions. At high potential gradients (≥ 1000 V) kinetic

emission of electrons by ion bombardment probably occurs.

Assuming a gain of 10^4 for eight dynodes and an electron-emission co-

efficient of 2 per incident ion, it is estimated that $\approx 1\%$ of Kr^* atoms having

13.5 to 14.0 eV of electronic excitation energy were ionized at the cathode.

This observation is consistent with previous work on surface-induced ionization

of metastable atoms at a surface.[40]

ACKNOWLEDGMENTS

FOOTNOTES AND REFERENCES

*Work done under auspices of the U. S. Atomic Energy Commission.

†Present address: The Culham Laboratory, Abindgon, Berkshire, England.

1.   W. Shottky, Phys. Z. 24, 350 (1923).

2.   H. W. Webb, Phys. Rev. 24, 113 (1924).

3.   See R. Dorrestein, Physica 9, 447 (1942) for early work, and Refs. 4 and

      5 for more recent work.

4.   W. Lichten, Phys. Rev. 120, 469 (1960).

5.   J. Olmsted, Amos S. Newton, and K. Street, J. Chem. Phys. 42, 2321 (1965).

6.   W. Lichten, J. Chem. Phys. 37, 2152 (1962).

7.   Robert S. Freund and William Klemperer, J. Chem. Phys. 47, 2897 (1967).

8.   W. Lichten, Phys. Rev. 120, 848 (1960).

9.   W. Lichten, J. Chem. Phys. 26, 306 (1957).

10.   A triode ion pump (General Electric Model 22TP250) was used originally

      to pump the excitation chamber C. It was found, however, that a coupling

      existed between the ion pump and the electron multiplier detector which

      resulted in a noise level in the detector system equal to the signal

      being detected (N_2 beam). Further, the pump was the source of considerable

      H_2 when hydrocarbons were pumped.

11.   R. Clampit, in Proceedings of 14th ASTM Conference on Mass Spectrometry,

      Dallas, 1966, p. 658.

12.   Manufactured by American Time Products, N. Y.

13.   Linde SHe-8 cryosorption pump.

14.   Varian Associates.

15.   Electronics Associates Incorporated.

16.   Robert S. Freund and William Klemperer, J. Chem. Phys. 43, 2422 (1965).

17. Olmsted found the O_2 or H_2O in the residual vacuum of his apparatus resulted in electron ejection from a Cs surface when struck by an O_2 or H_2O molecule. This effect increased considerably the noise level of the detector as well as shortening the useful lifetime of the surface.

18. ITT Industrial Laboratories, Phototube FW141.

19. R. E. Fox, W. M. Hickam, D. J. Grove, and T. Kjeldaas, Jr., Rev. Sci. Instr. 26, 1101 (1955).

20. Princeton Applied Research, Model HR-8.

21. Michiyuki Nakamura, Frederick E. Vogelsburg and W. Larry Crowder, in Nuclear Chemistry Division Annual Report, 1966, UCRL-17299, January 1967, p. 358.

22. P. Warmek, Discussions Faraday Soc. 37, 57 (1964).

23. H. Beutler and H. O. Jünger, Z. Phys. 101, 285 (1936).

24. V. Čermák, J. Chem. Phys. 44, 1318 (1966).

25. M. Leventhal, R. T. Robiscoe, and K. R. Lea, Phys. Rev. 158, 49 (1967).

26. R. F. Stebbings, Wade L. Fite, David G. Hunnes, and R. T. Brackman, Phys. Rev. 119, 1939 (1960).

27. G. M. Prok, C. F. Monnin, and H. J. Hettel, NASA Report TN-D-4004-1967.

28. H. H. Brongersma and L. J. Oosterhoff, Chem. Phys. Letters 1, 169 (1967).

29. Ernst Teloy, Dissertation, Rheinischen Friedrich-Wilhelms-University, Bonn, 1965.

30. G. E. Hansche, Phys. Rev. 57, 289 (1940).

31. A reevaluation of Hansche's data plus the observations by Olmsted, Newton, and Street (Ref. 5), indicates that the half-life of the transition $a^3\Pi_r \to X^1\Sigma^+$ in CO is between 30 and 80 μsec, with a most probable value of 40 ± 10 μsec. The work of Freund and Klemperer (Ref. 16) shows the half life to be greater than 500 μsec.

32. H. Ehrhardt and K. Willmann, Z. Physik 204, 462 (1967).

33. P. T. Stewart and E. Gabathuler, Proc. Phys. Soc. (London) 72, 287 (1958).

34. H. F. Winters, J. Chem. Phys. 43, 926 (1965).

35. RCA photomultiplier, type 931A.

36. J. Olmsted III, Radiation Res. 31, 191 (1967).

37. J. T. Tate and P. T. Smith, Phys. Rev. 46, 773 (1934).

38. A. Kuppermann and L. M. Raff, Discussions Faraday Soc. 35, 30 (1963).

39. J. P. Doering, J. Chem. Phys. 46, 1194 (1967).

40. Amos S. Newton, A. F. Sciamanna, and R. Clampitt, J. Chem. Phys. 46, 1779 (1967).
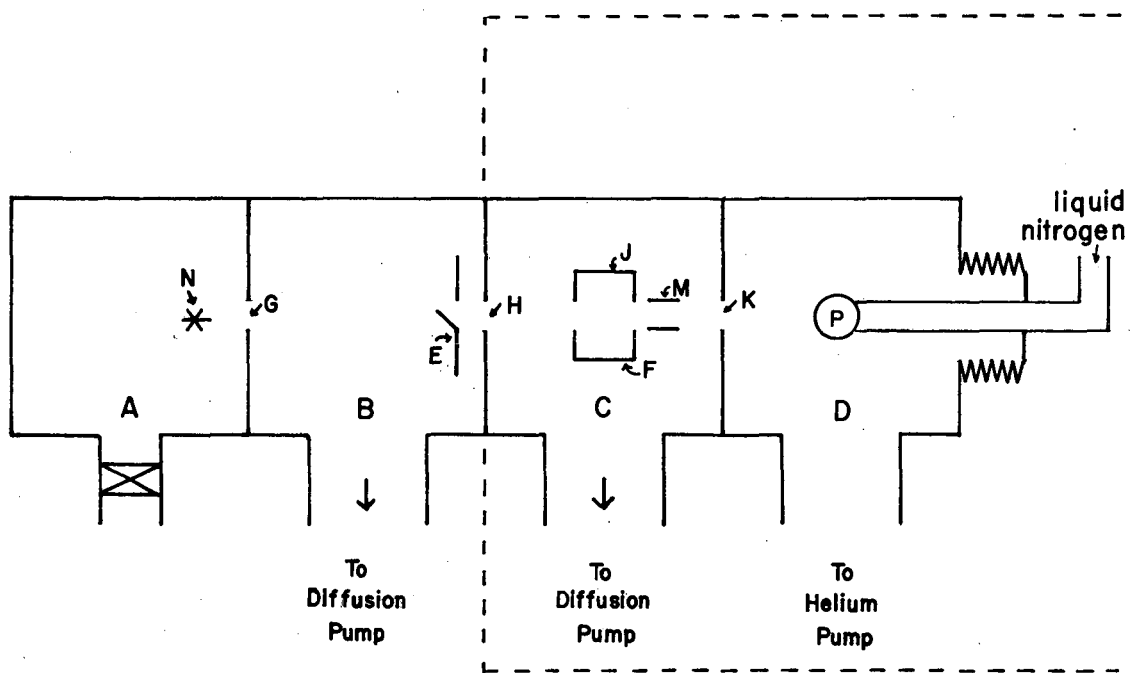
XBL 6712-6293

Fig. 1. Schematic diagram of molecular beam apparatus for study of long-lived excited states of atoms and molecules.
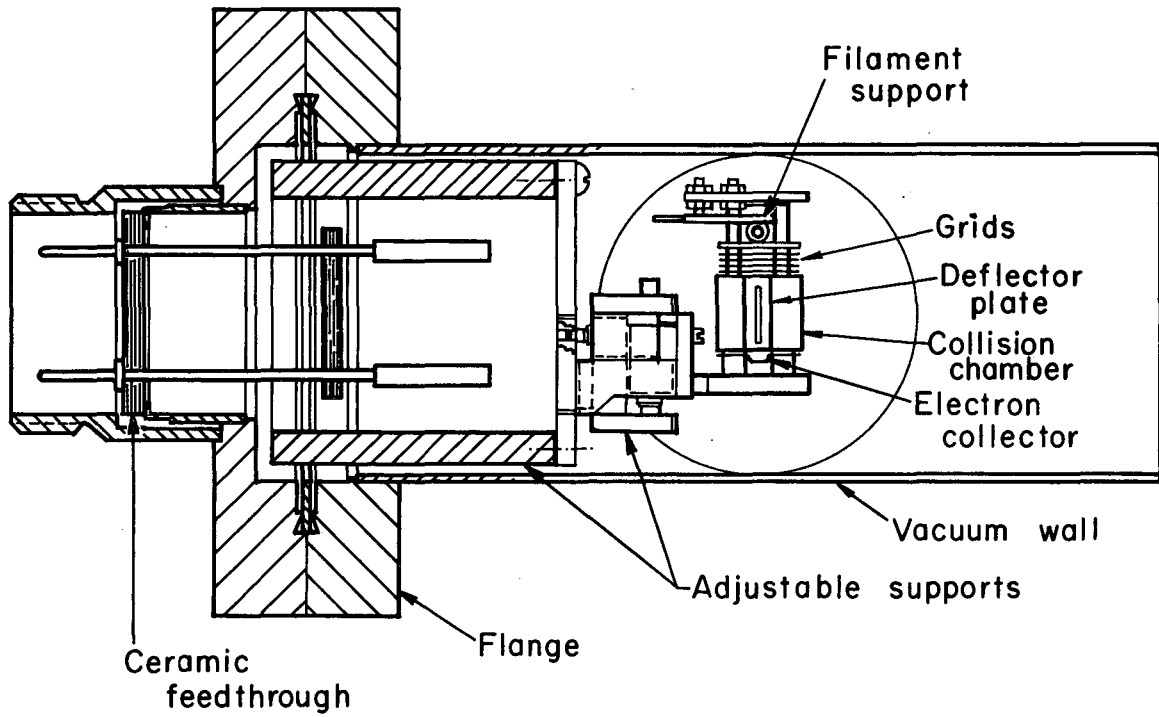
XBL6712-5759

Fig. 2.   The electron gun and its supports.
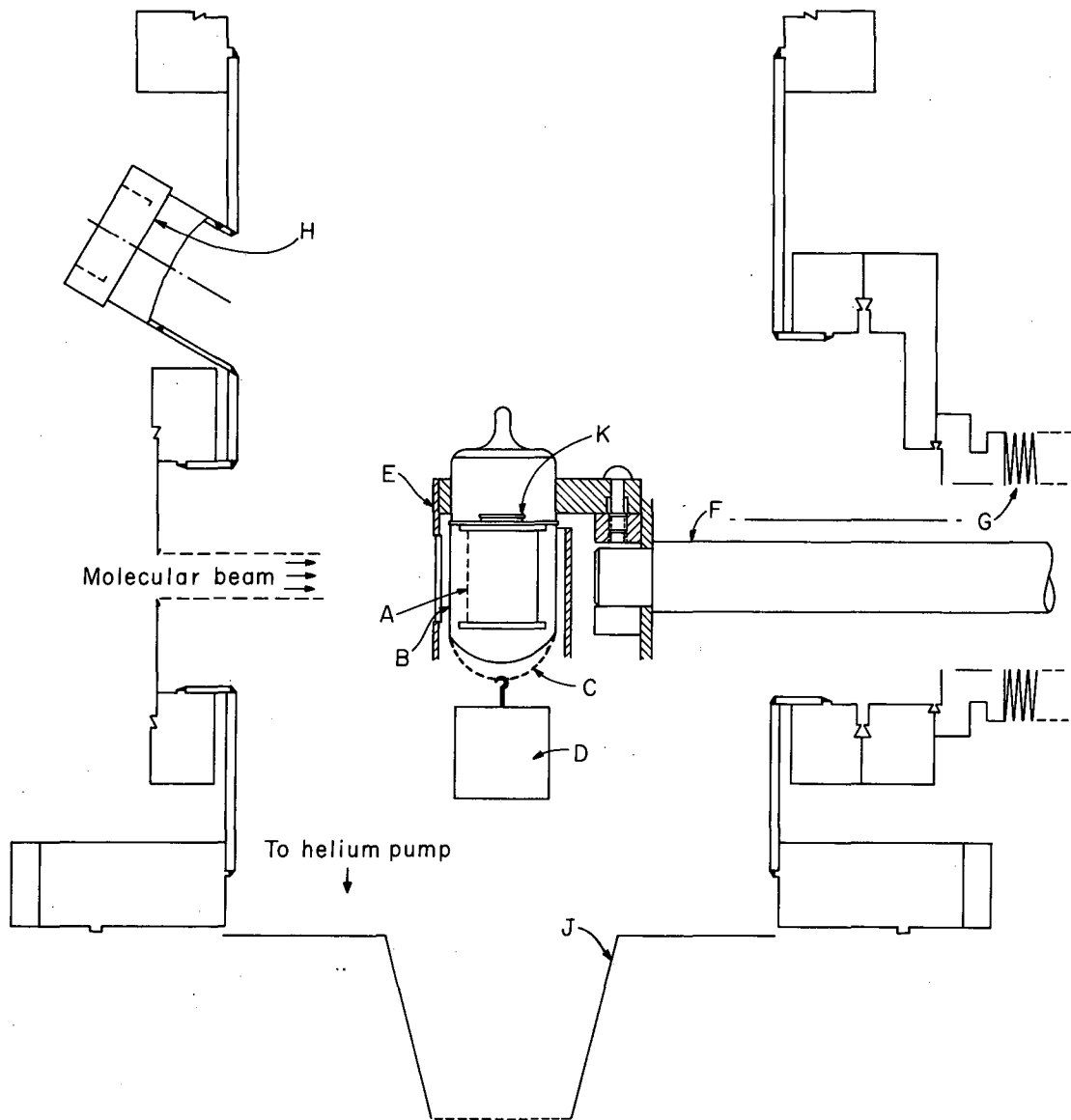
Fig. 3. Schematic diagram of the detector chamber. System for removal of
glass envelope from the photomultiplier in an ultrahigh vacuum.
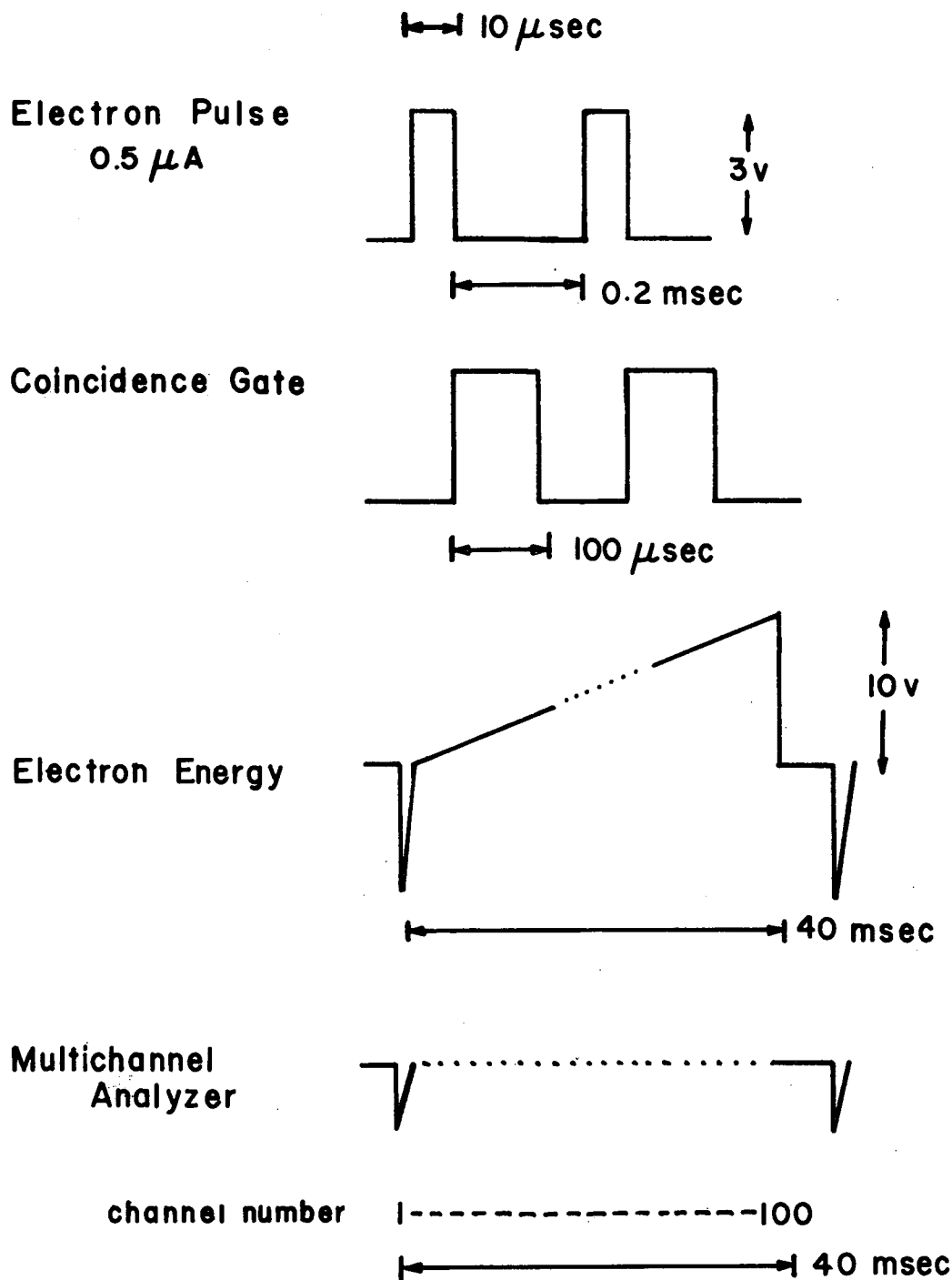
Fig. 4. Scheme of delayed coincidence counting for recording of the excitation
functions of excited species.
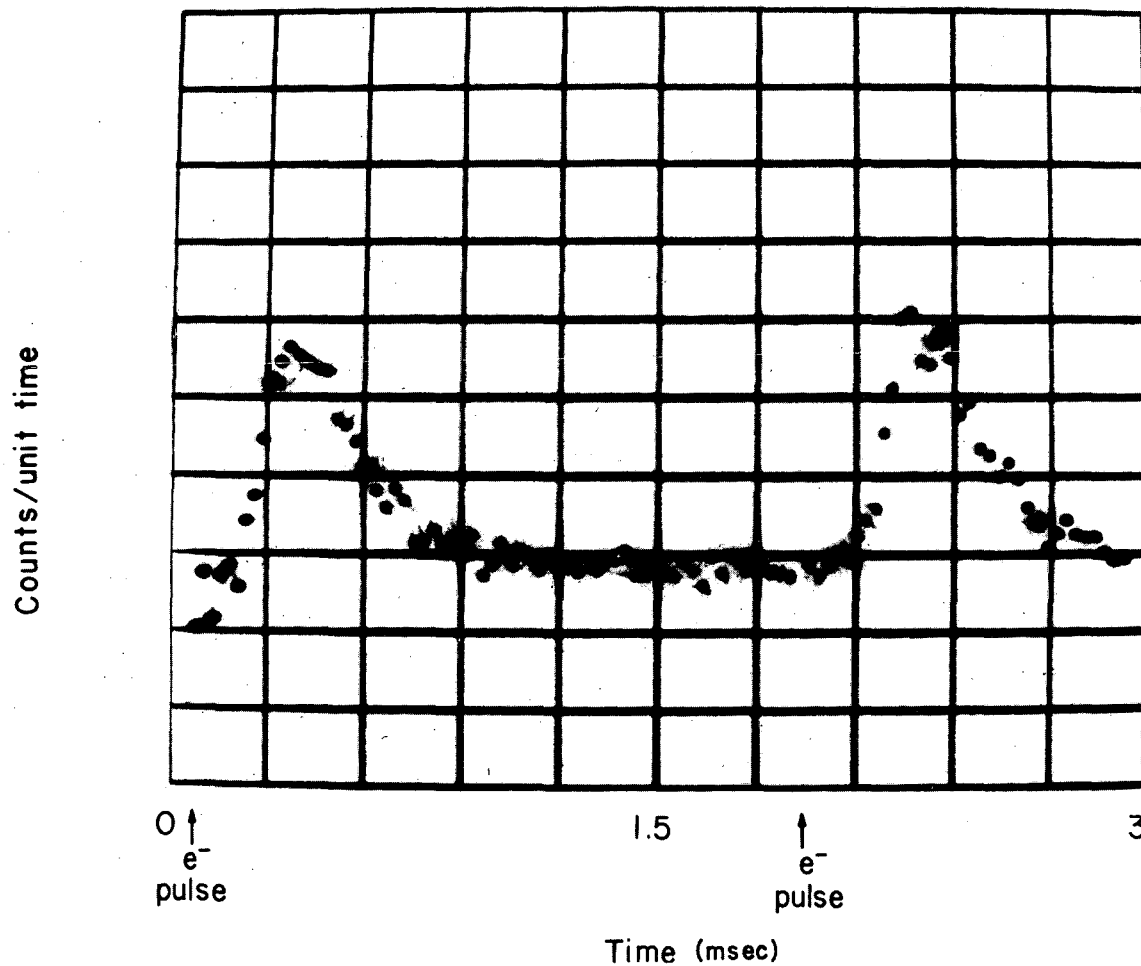
Fig. 5. Velocity distribution of Kr^* atoms produced by electron impact on Kr: 20-μsec pulse, 17-eV electrons; 3 msec full scale; one electron pulse every 2 msec. Two electron pulses are shown.
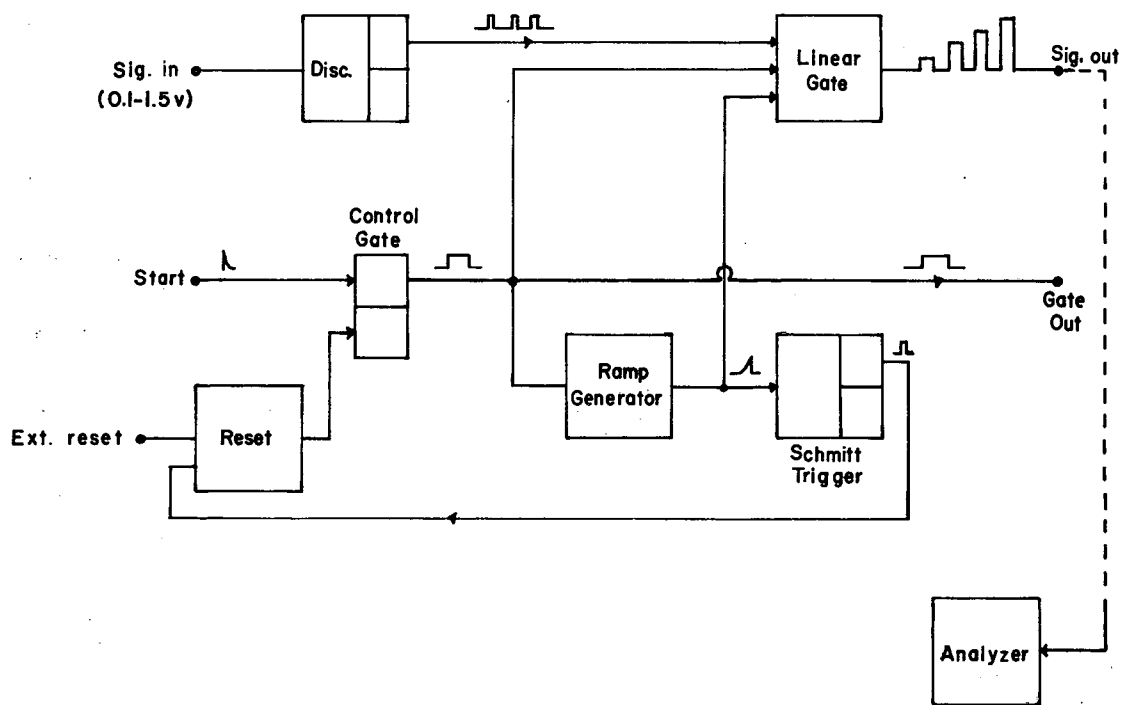
Fig. 6. Scheme for studying excited species arriving at the detector 1 μsec or longer after excitation.
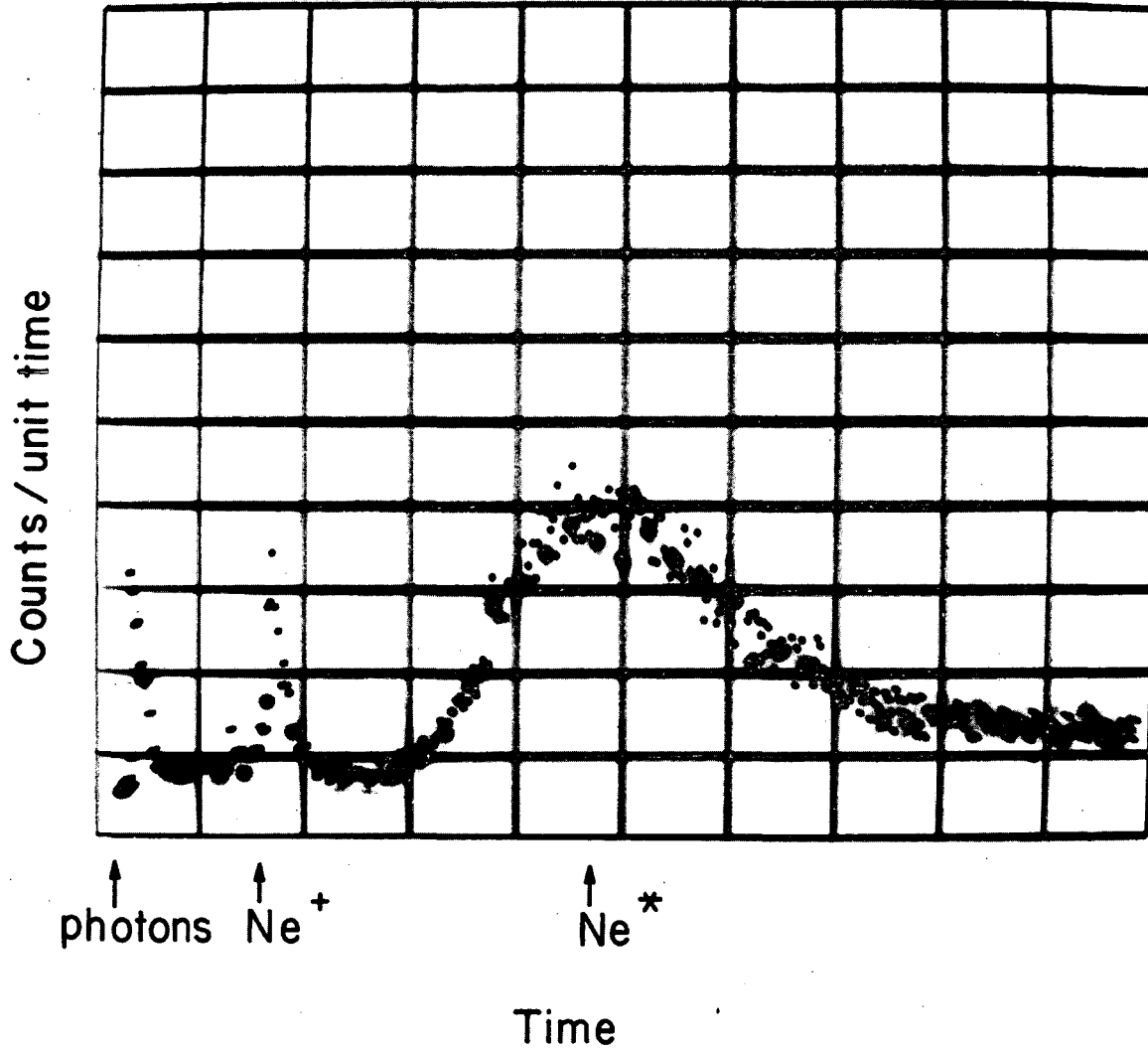
Fig. 7. Time-of-flight resolution of photons, Ne^+ ions, and Ne^* atoms pro-
    duced by electron impact on neon: 10-μsec pulse, 23-eV electrons; 400 μsec
    full scale.
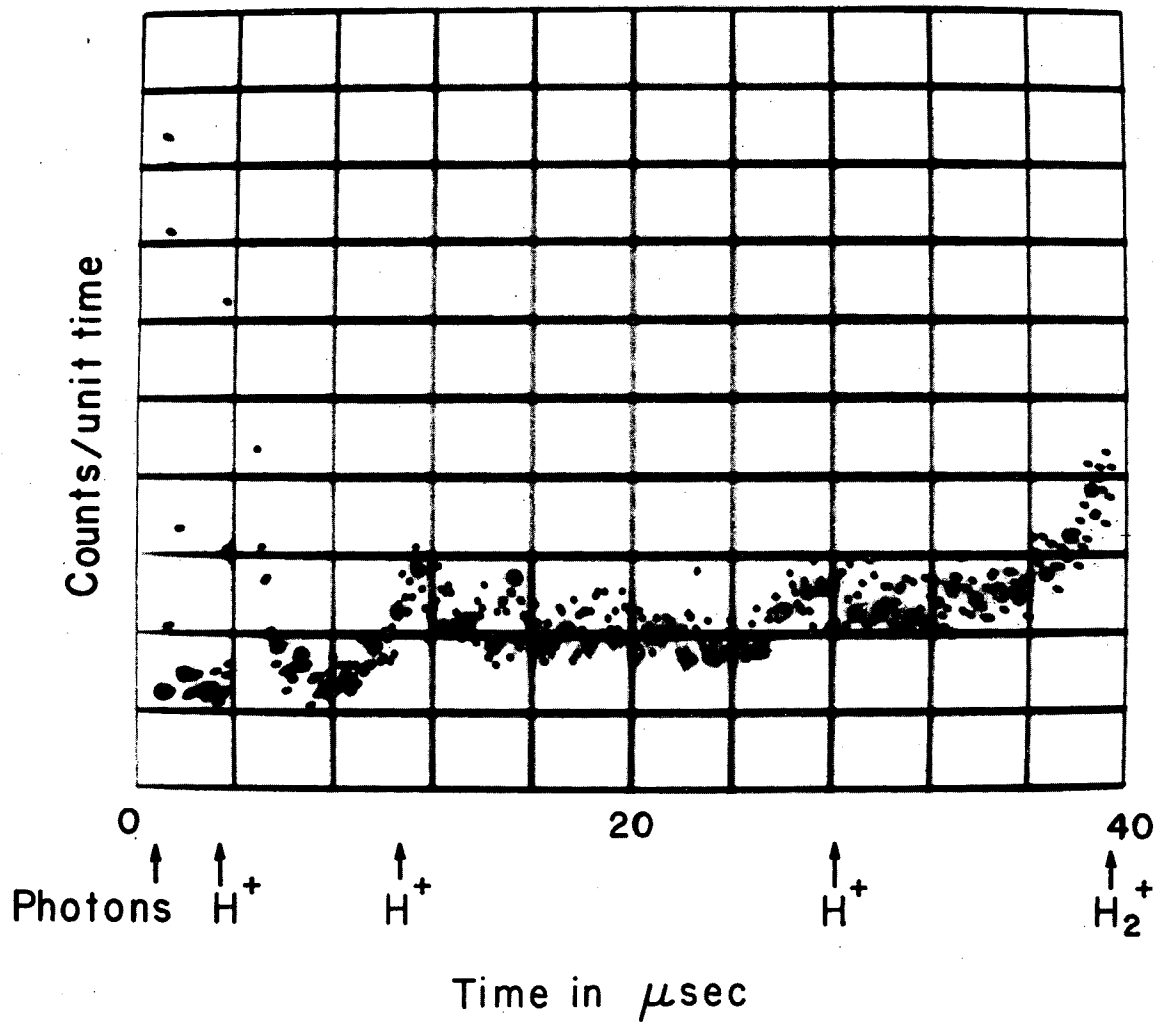
XBB 6712-6865

Fig. 8. Time-of-flight resolution of photons, H^+ ions and H_2^+ ions produced by electron impact on hydrogen: 0.5-µsec pulse, 38-eV electrons; 40 µsec full scale.
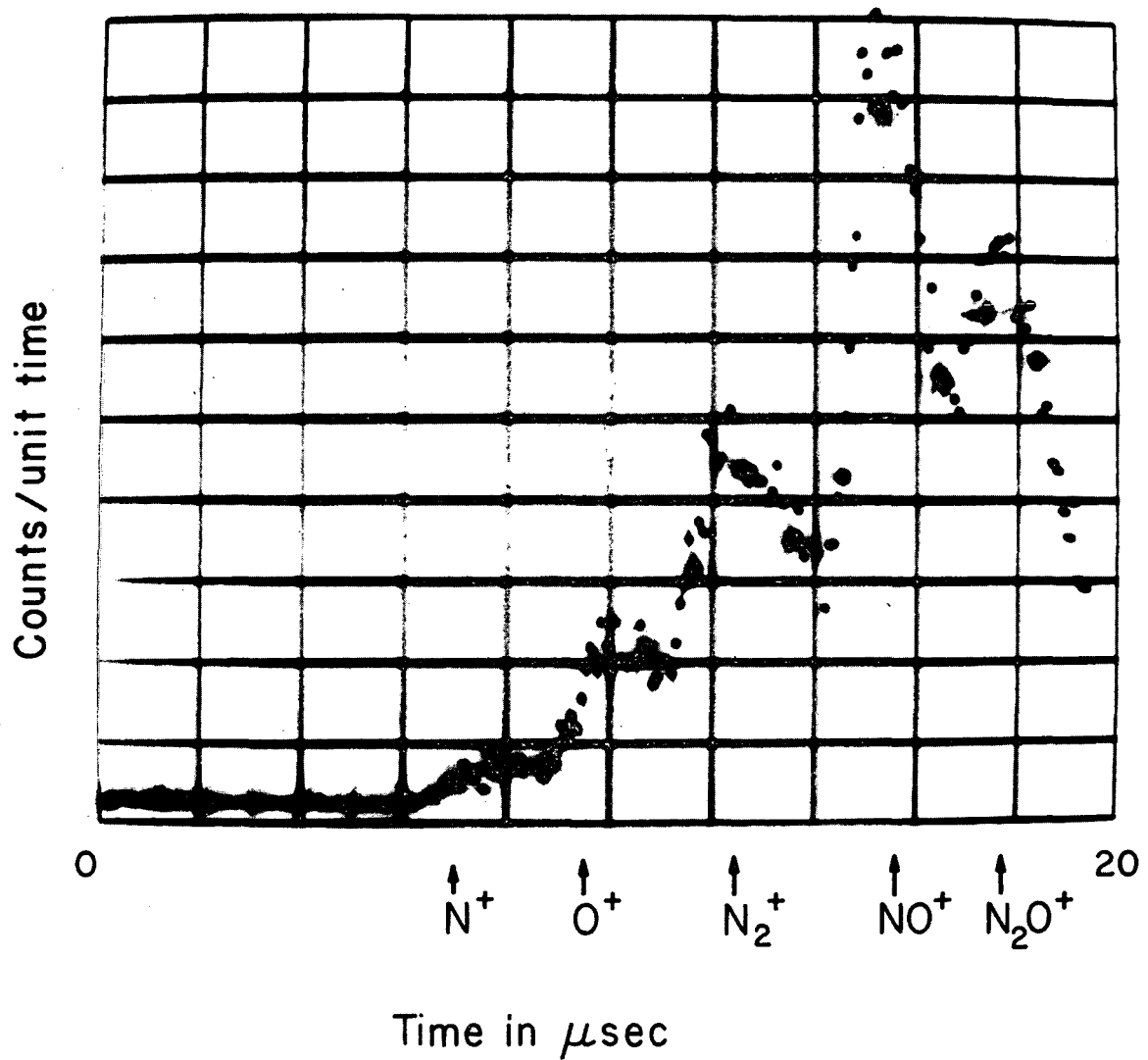
Fig. 9. Time-of-flight resolution of positive ions produced by electron impact on N_2O: 10-μsec pulse, 30-eV electrons; 20 μsec full scale.
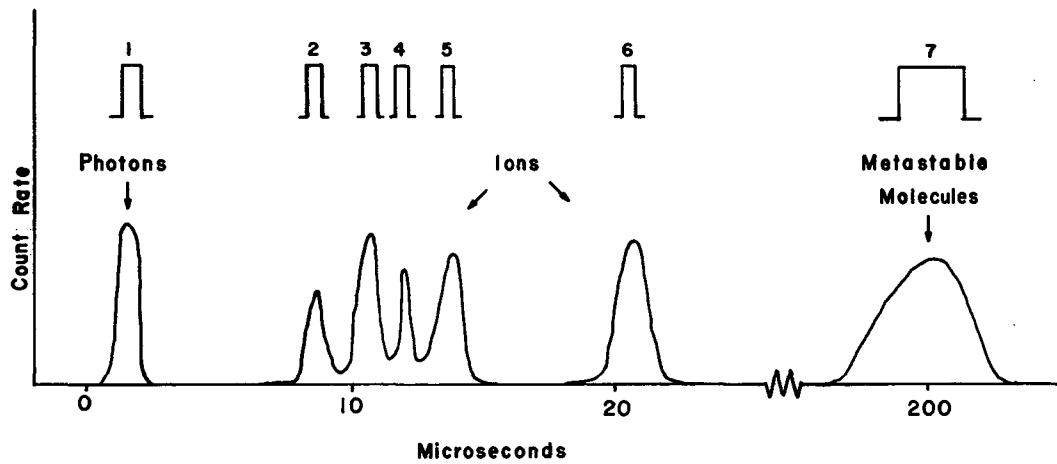
XBB 6712-6858

Hypothetical time of flight distribution of species produced by electron impact on a molecule

Fig. 10. Hypothetical time-of-flight distribution of species produced by electron impact on a molecule.
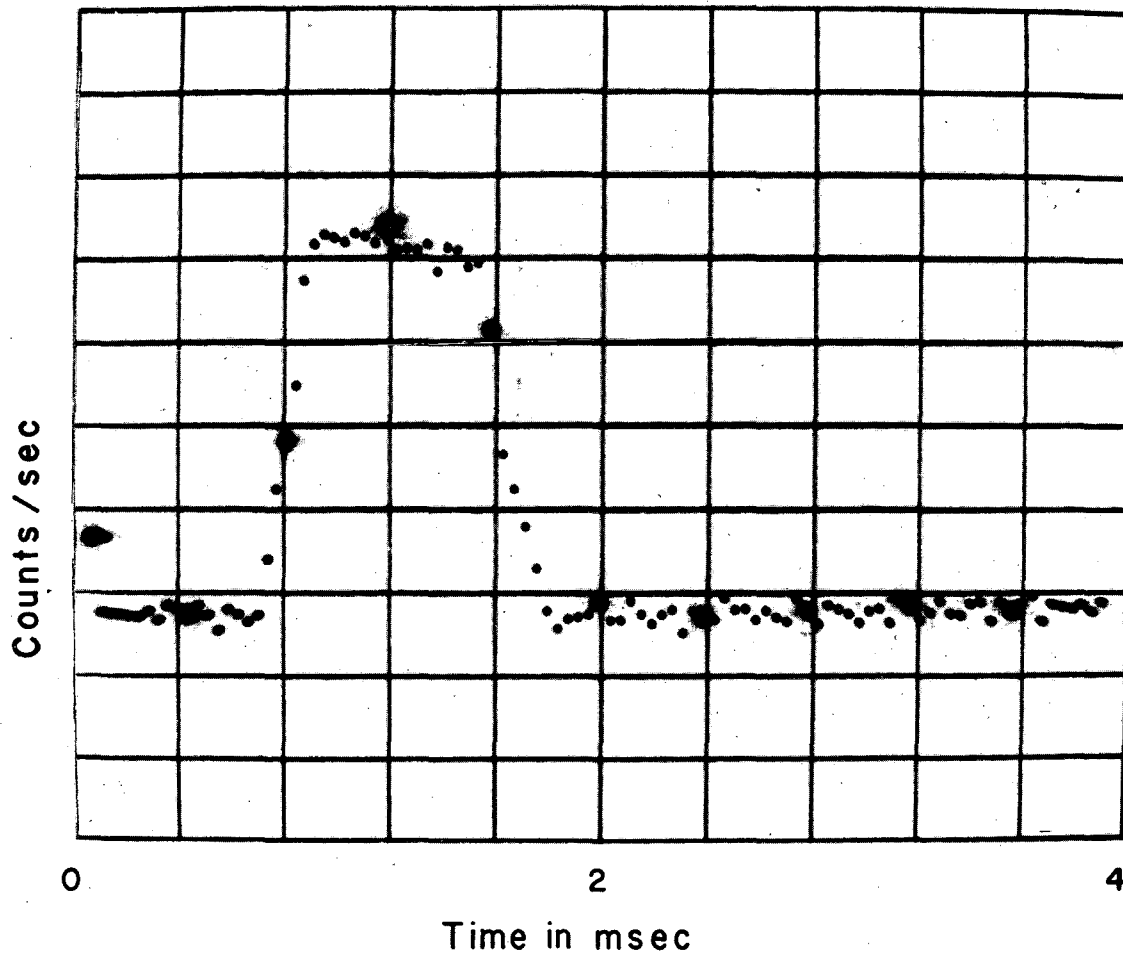
XBB 6711-6582

Fig. 11. Profile of the light passing through the slit produced by the mechanical chopper. Chopper is open for 1 msec.
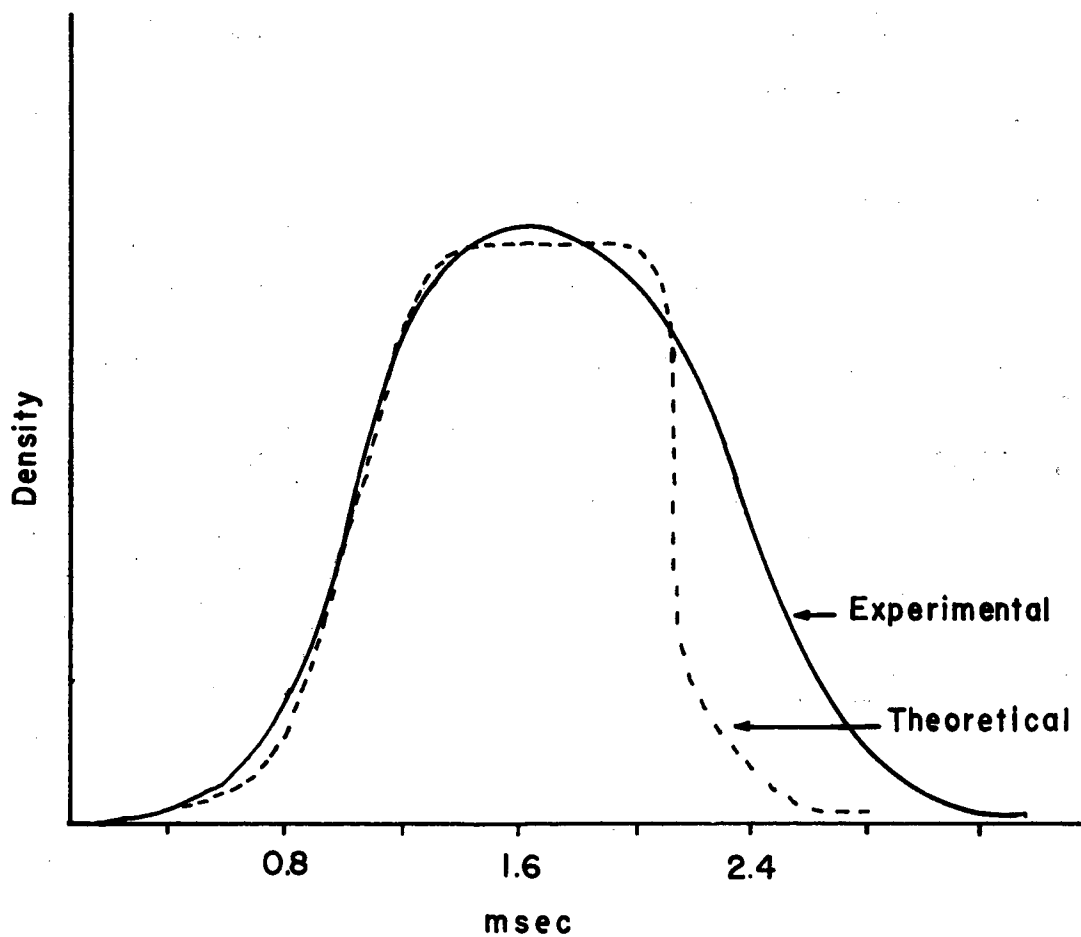
Fig. 12. Calculated and observed intensity profiles of Kr* atoms formed in a
molecular beam of Kr which is modulated at a trapezoidal slit. Open time
of slit is 1 msec.
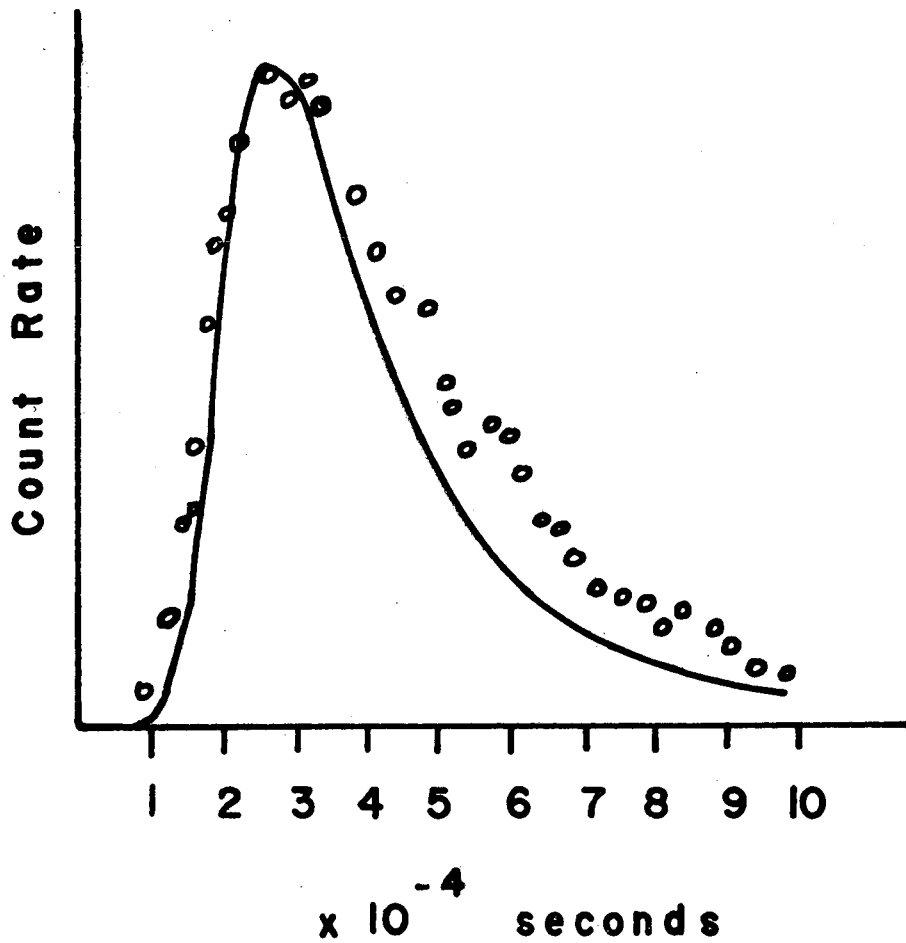
XBL 6712-6298

XBL 6712-6297

Fig. 12a. Velocity distribution of Ar atoms in a molecular beam excited by a
30 μsec electron pulse. Abcissa is the time of arrival at detector after
the electron pulse. The curve is calculated from Eq. 4., points are
experimental.
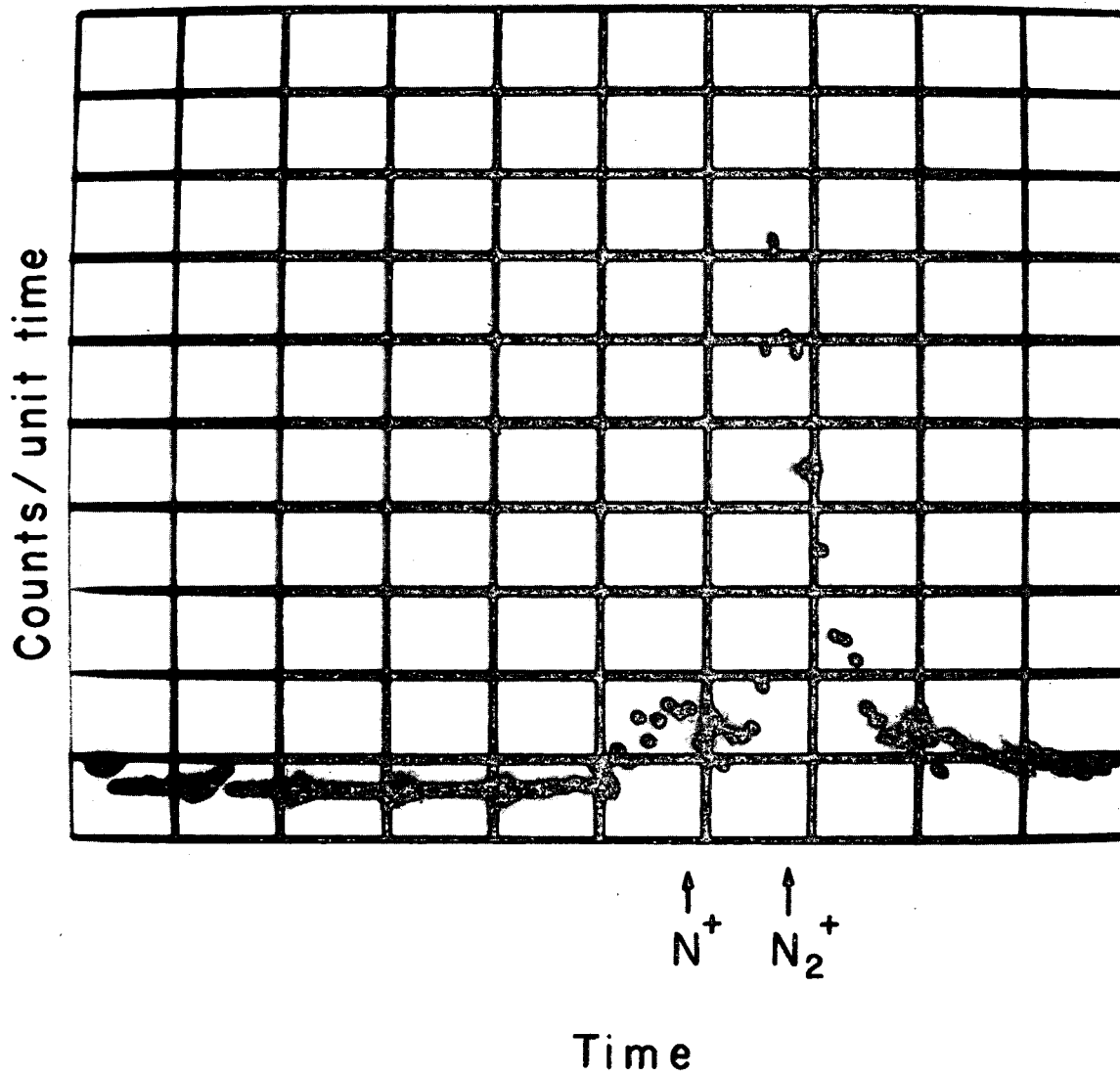
Fig. 13. Time-of-flight resolution of ions produced by electron impact on N_2: 5-µsec pulse, 24-eV electrons; 25 µsec full scale.
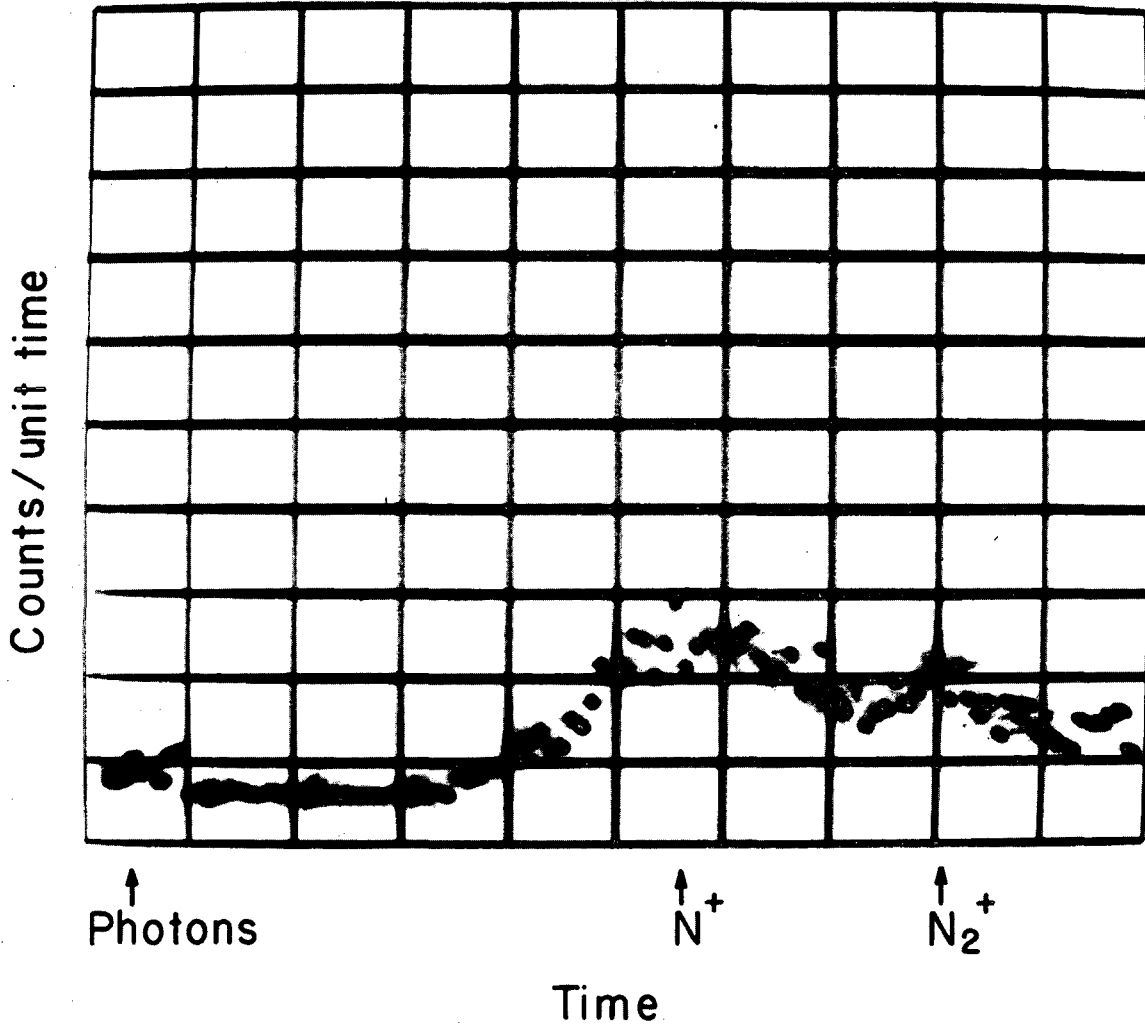
XBB 6712-6862

Fig. 14. Time-of-flight resolution of ions produced by electron impact on N_2: 5-μsec pulse, 35-eV electrons; 25 μsec full scale.
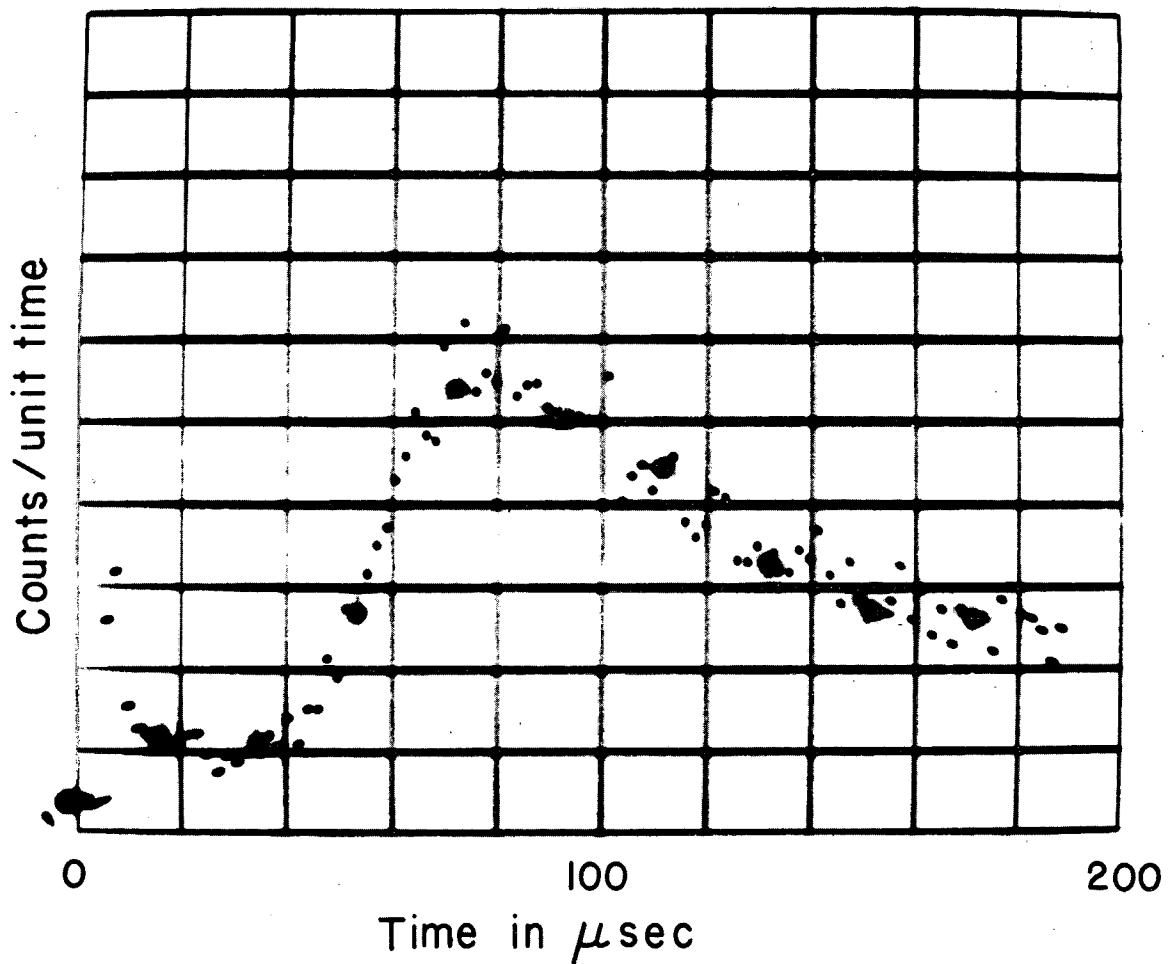
Fig. 15. Velocity distribution of excited neutral fragments produced by
    electron impact on N_2O: 9-μsec pulse, 25-eV electrons; 200 μsec full scale.
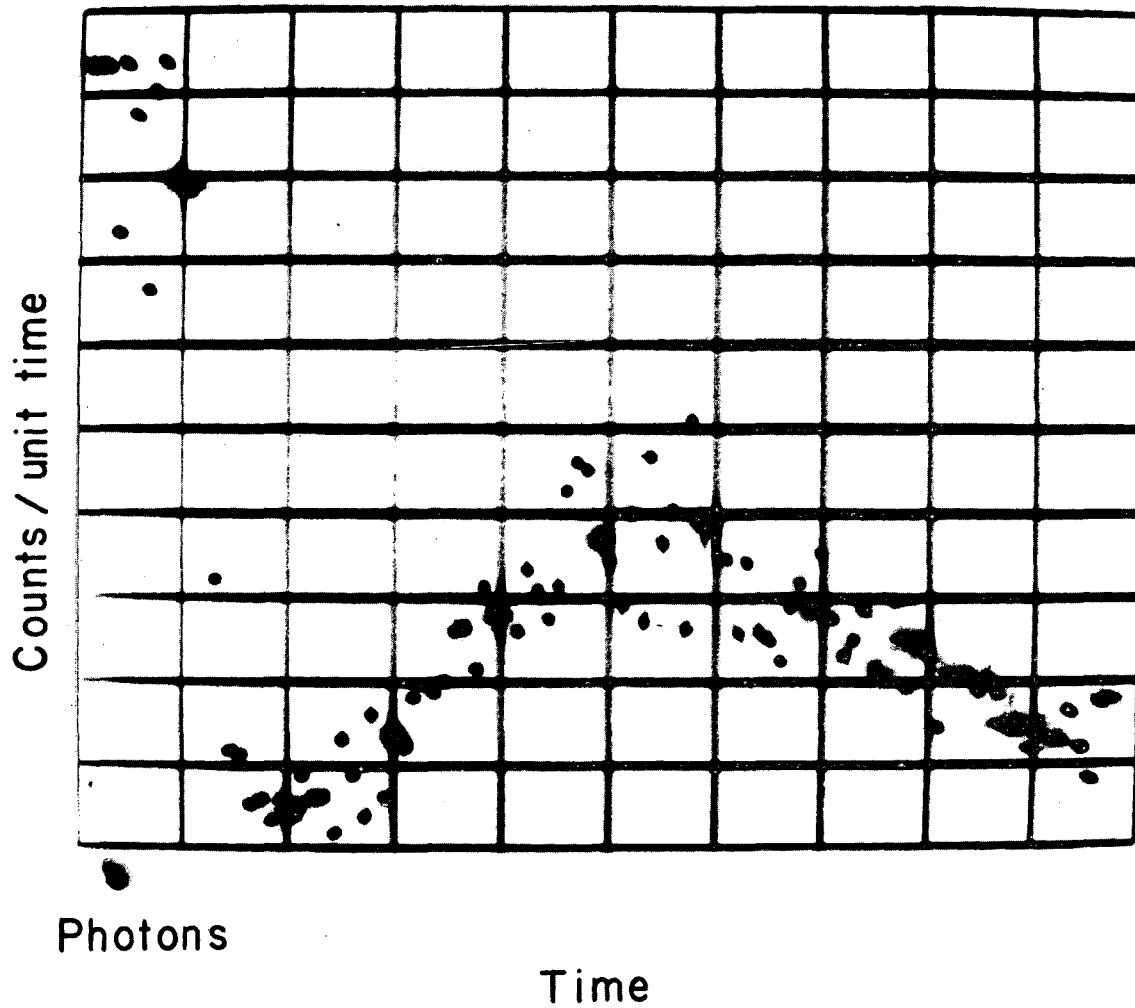
Fig. 16. Time-of-flight resolution of photons and excited neutral fragments pro-
duced by electron impact on CO_2: 30-μsec pulse, 30-eV electrons, 200 μsec
full scale. Photon counts are off scale.
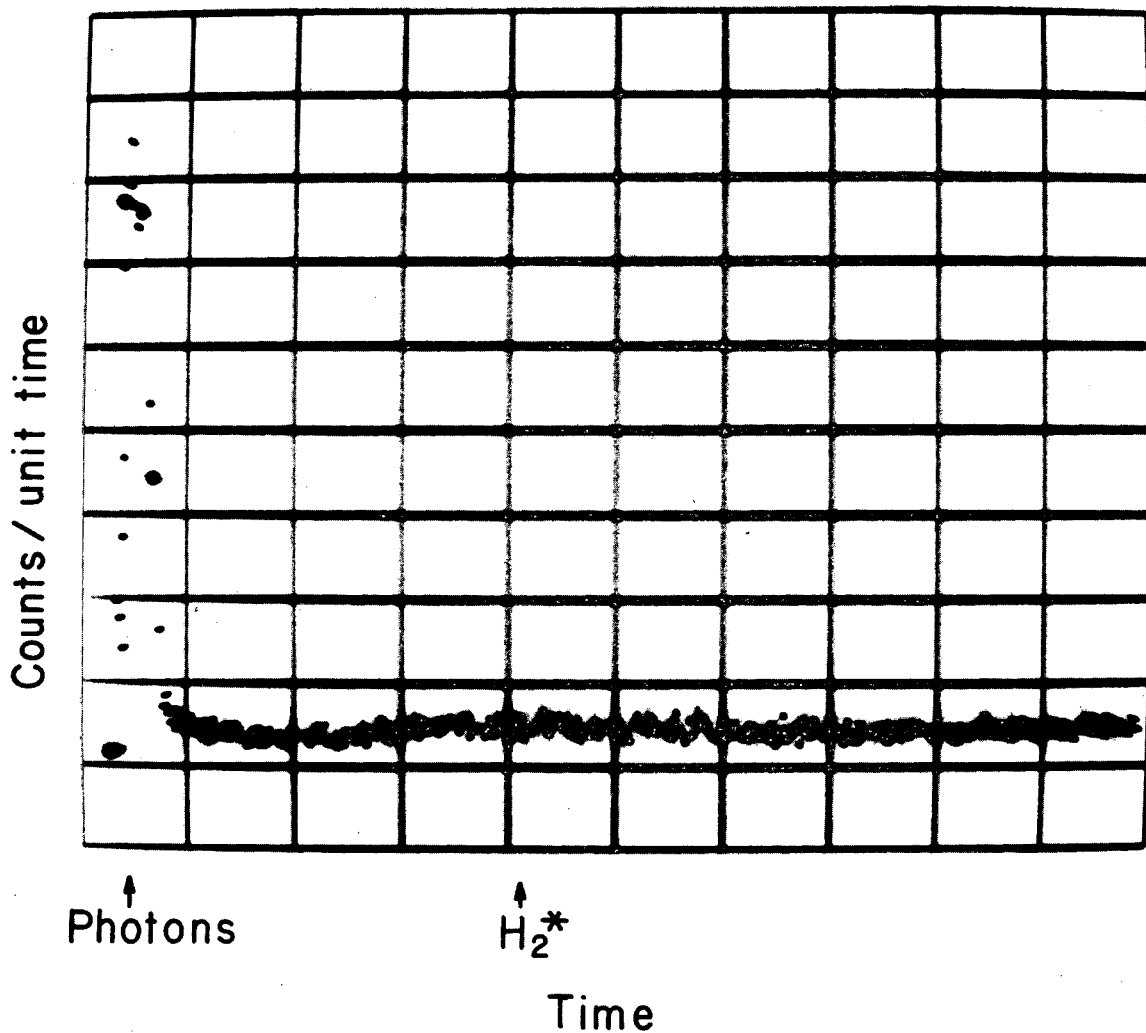
XBB 6712-6853

Fig. 17. Time-of-flight resolution of photons and metastable molecules produced by electron impact on H_2: 5-μsec pulse, 19.5-eV electrons; 200 μsec full scale. The signal from H_2^* is low because of the short counting time necessary to keep photon counts on scale.
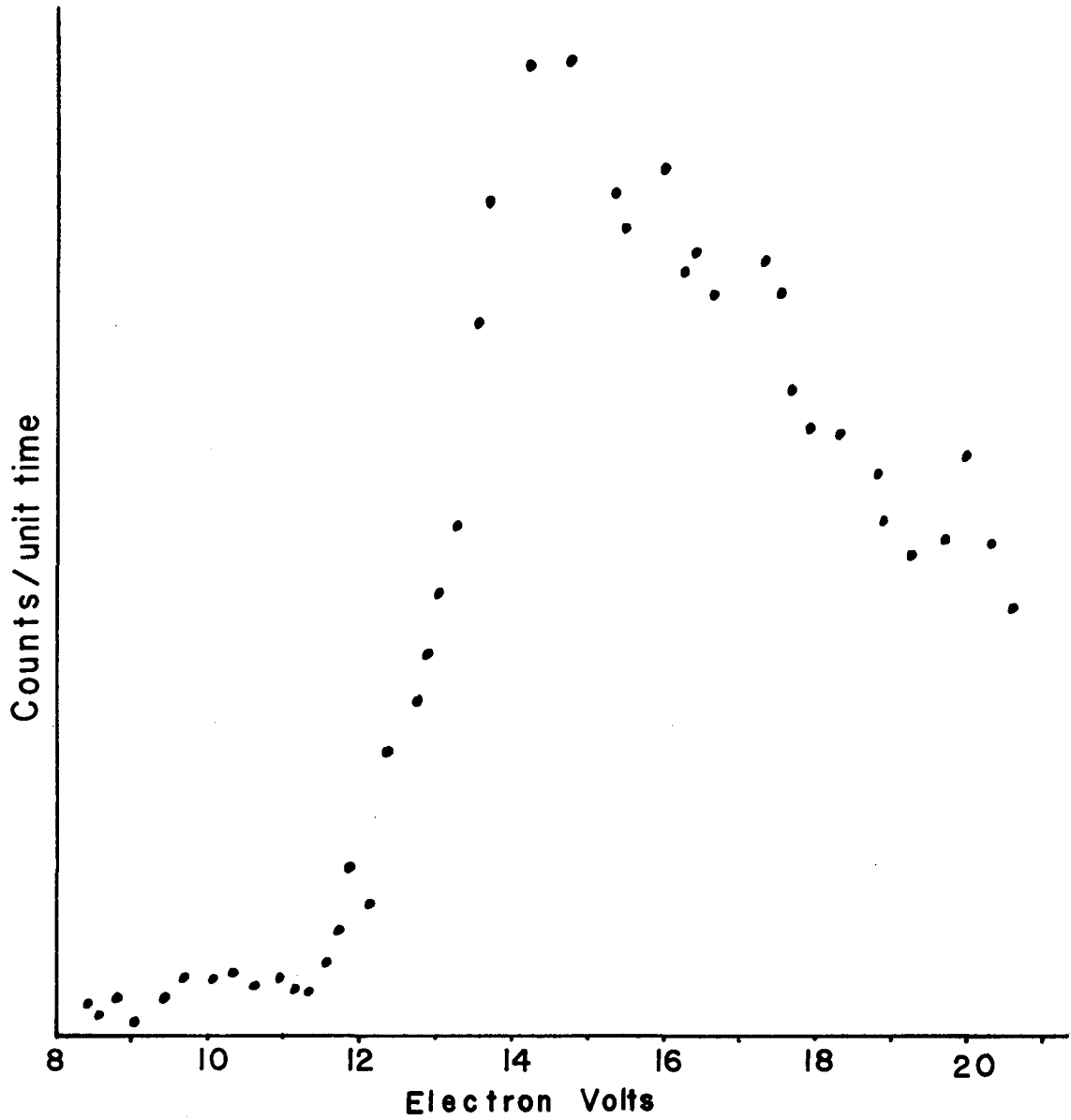
XBL 6712-1960

Fig. 18. Excitation curve for production of H_2^* by electron impact on H_2 (energy scale uncorrected).
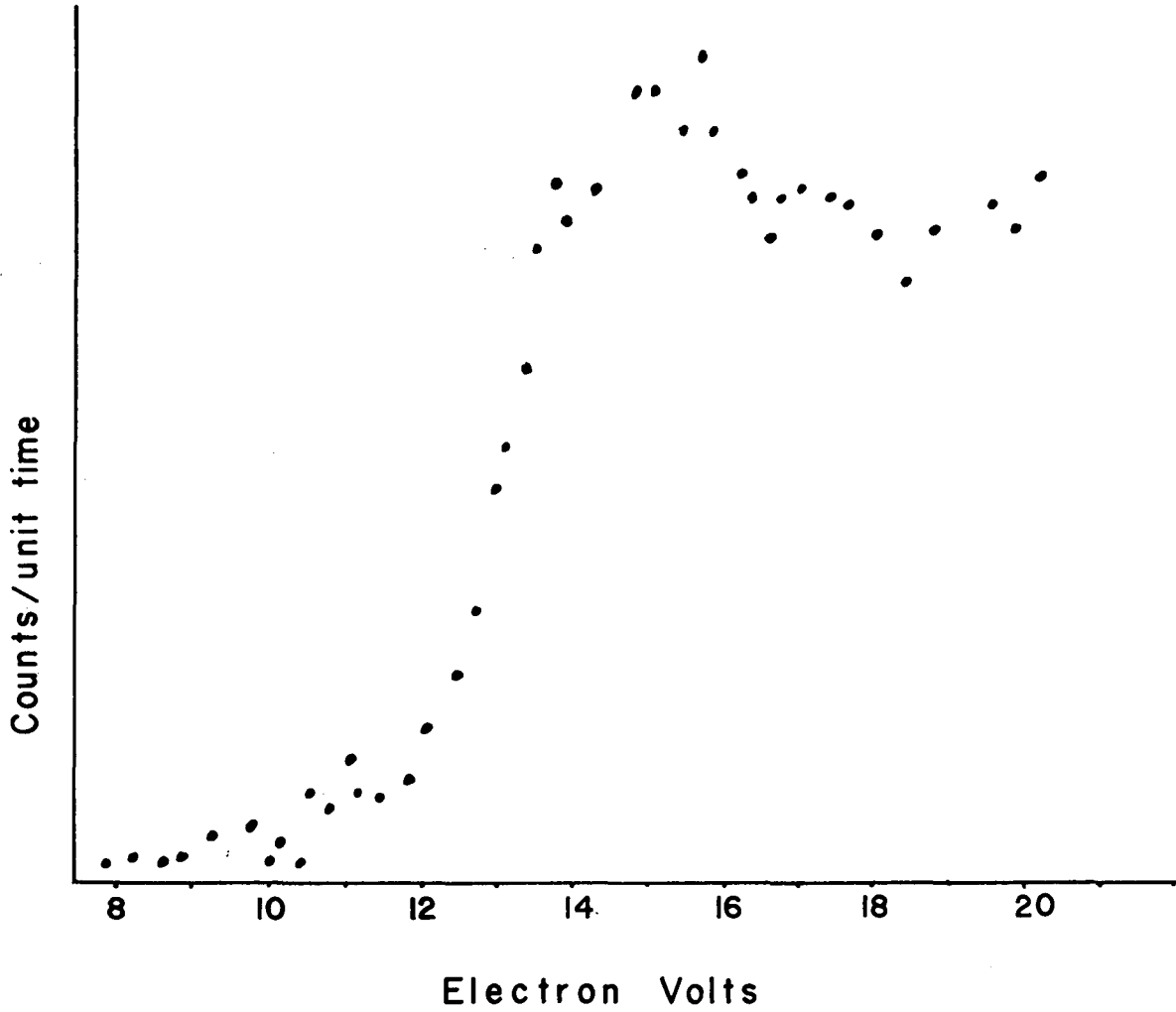
Fig. 19.   Excitation curve for production of photons by electron impact on H_2 (energy scale uncorrected).
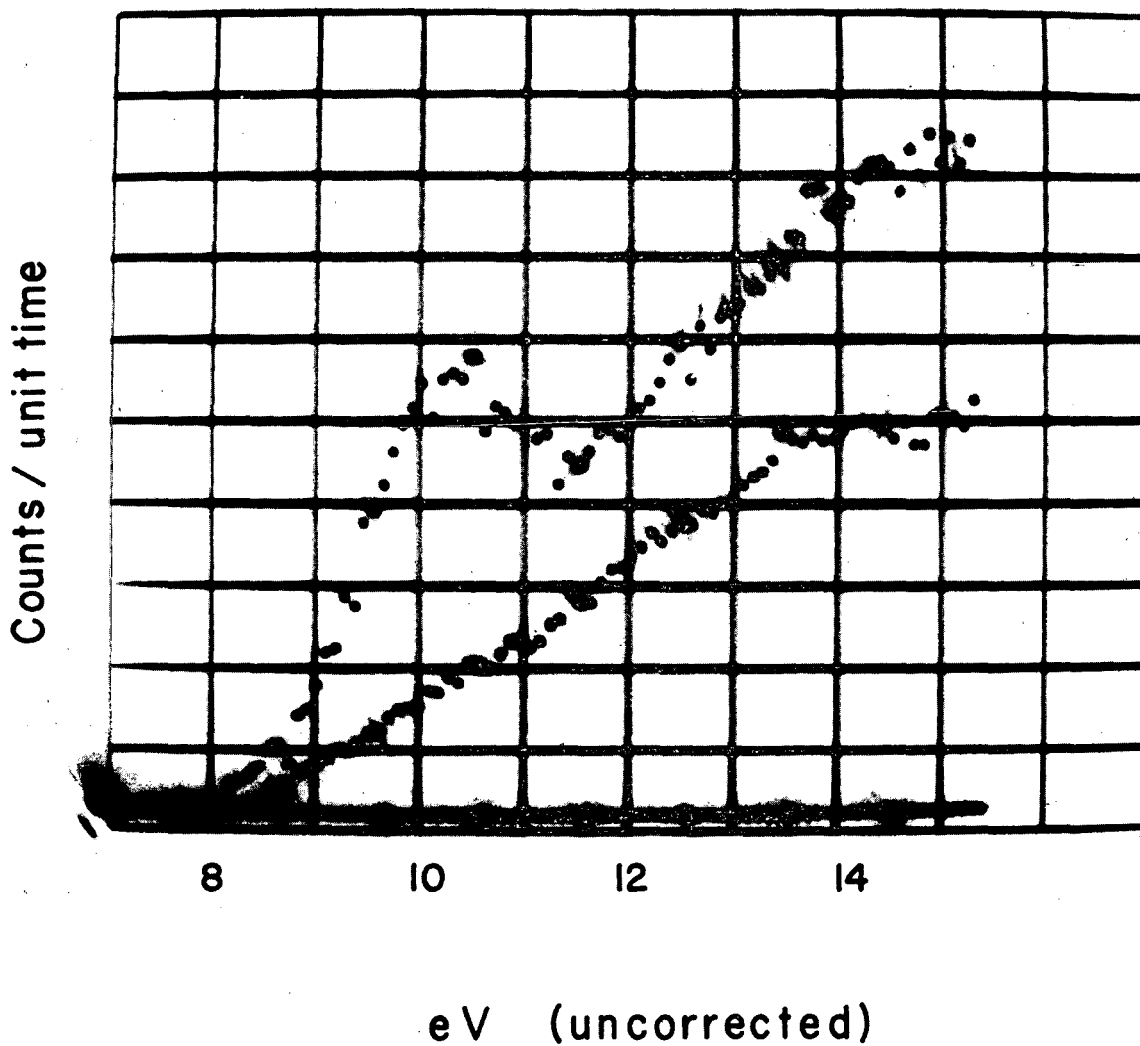
XBB 6712-6868

Fig. 20. Excitation curve for the production of CO* (upper curve) and Kr* (lower curve) by electron impact on CO and Kr respectively. Energy scale for Kr* production is displaced on abscissa by ≈ 3 eV. Note the resonance peak in the CO* curve at 10.5 eV.
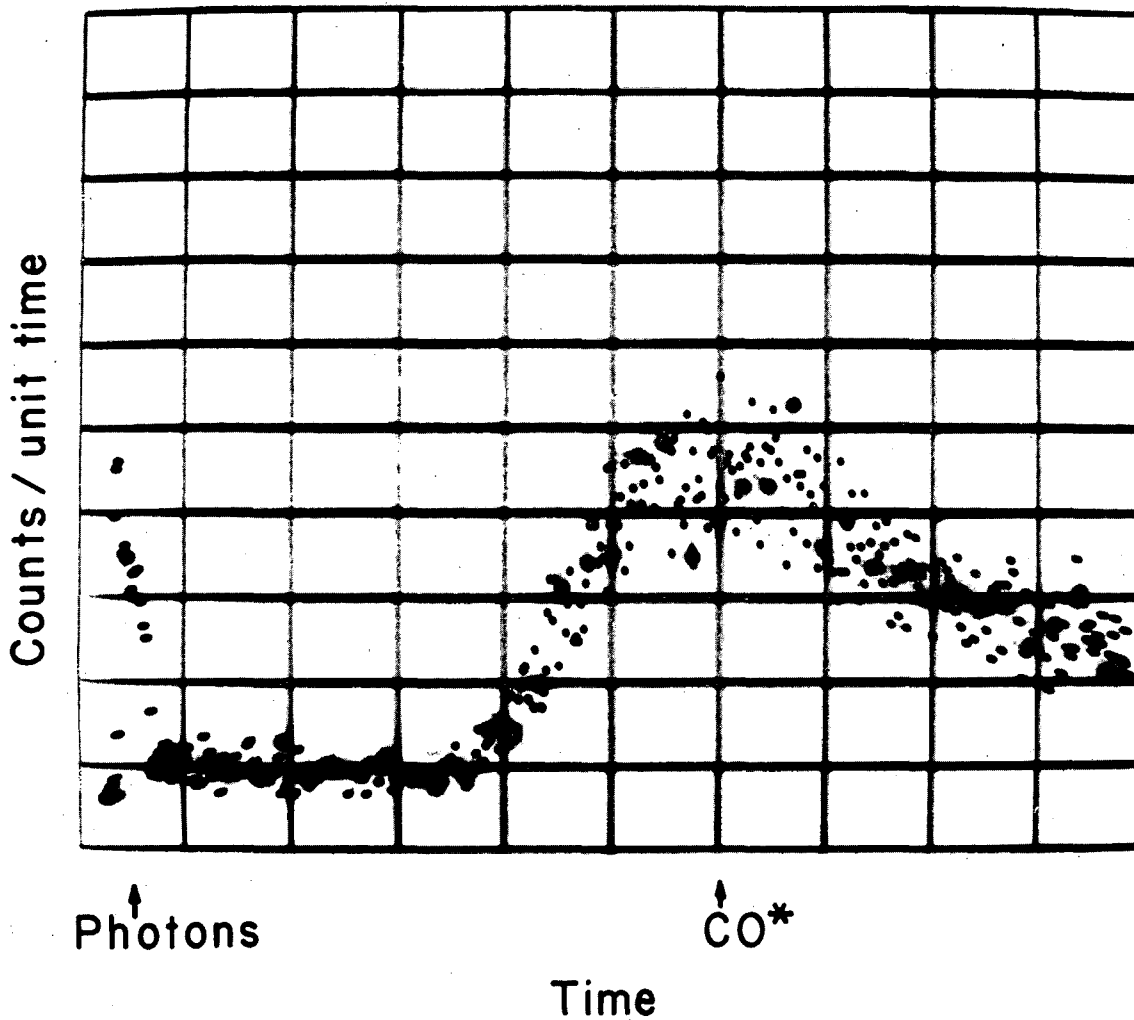
Fig. 21. Time-of-flight resolution of photons and CO* produced by electron impact on CO: 15-μsec pulse, 15-eV electrons; 400 μsec full scale.
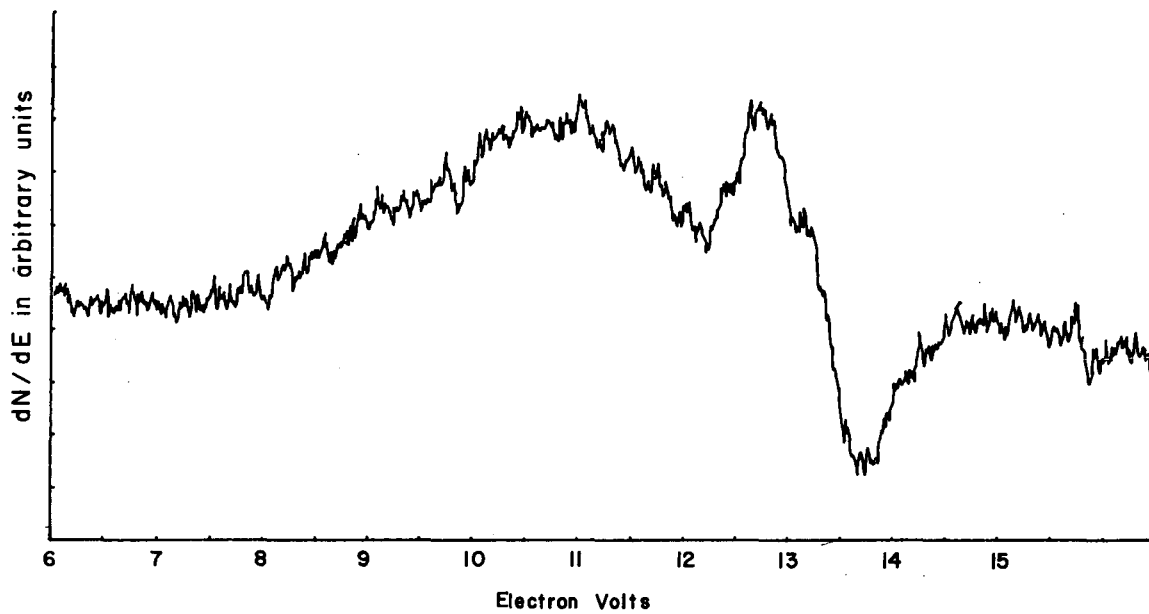
XBL 6712-1955

Fig. 22. First differential of excitation curve for production of N_2^* by electron impact on N_2: antimony detector, energy scale uncorrected.
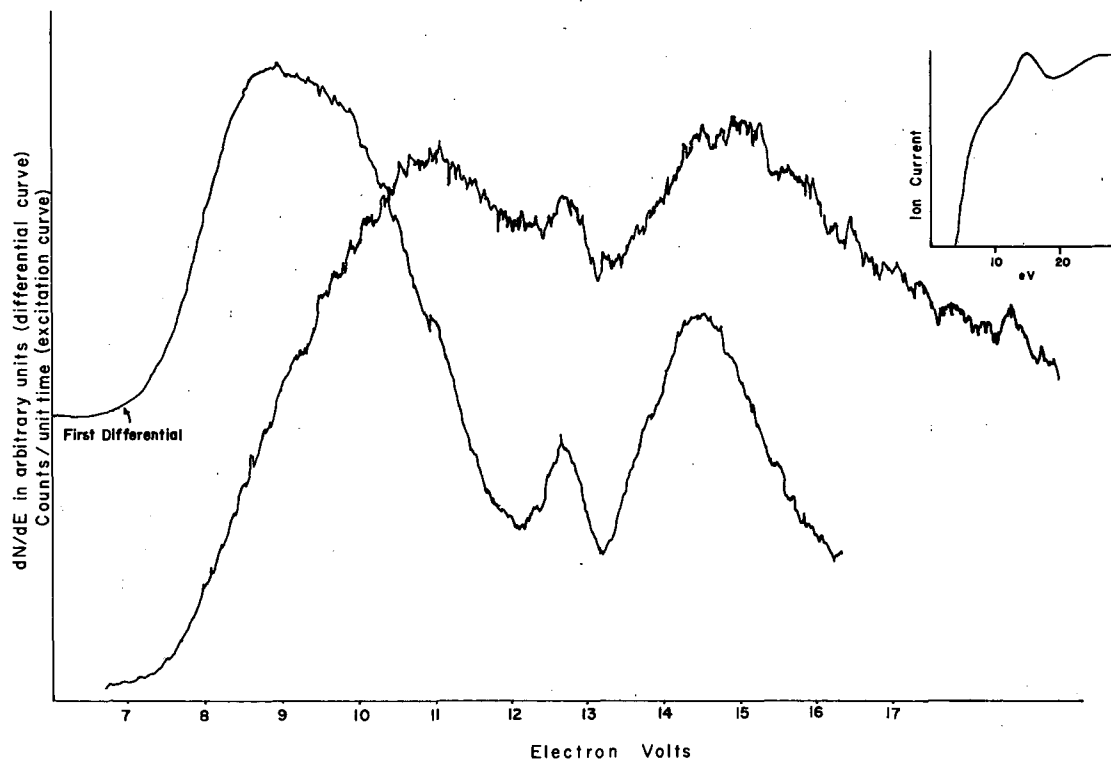
Fig. 23. Excitation curve and its first differential (so designated) for the production of N_2^* by electron impact on N_2: detector, cesium surface on antimony base; energy scale uncorrected. Inset: Ionization efficiency curve for the process: $Cs + e^- \rightarrow Cs^+ + 2e^-$.
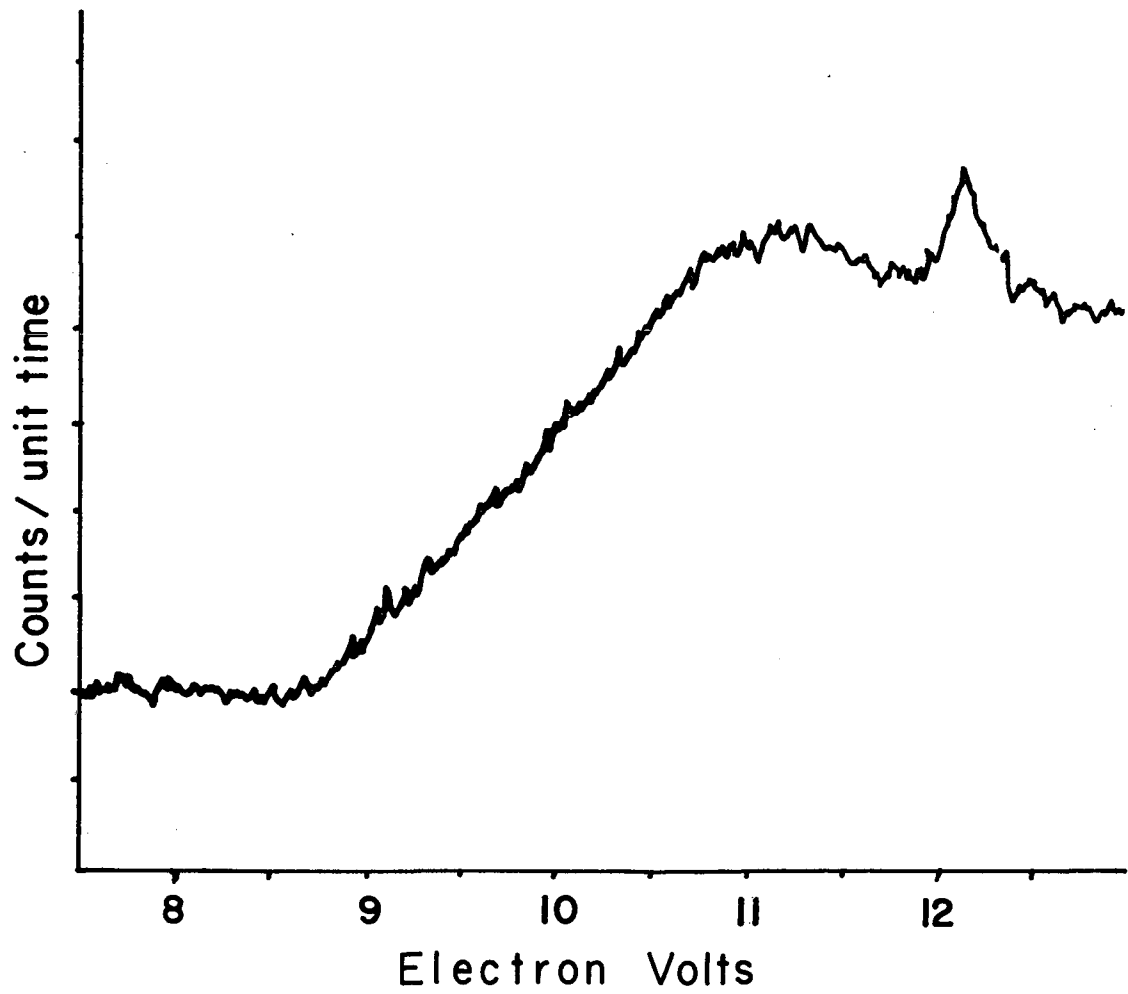
XBL 6712-1956

Fig. 24. Excitation curve for the production of N_2^* by electron impact on N_2: RPD method; Cs_3Sb detector, energy scale uncorrected.